DOKUZ EYLÜL UNIVERSITY
GRADUATE SCHOOL OF NATURAL AND APPLIED SCIENCES

INVESTIGATION OF EFFECT OF COATING TYPE ON CORROSION PERFORMANCE OF REINFORCEMENT BARS

by
Houman VAHEDI

October, 2019
İZMIR

INVESTIGATION OF EFFECT OF COATING TYPE ON CORROSION PERFORMANCE OF REINFORCEMENT BARS

A Thesis Submitted to the
Graduate School of Natural and Applied Sciences of Dokuz Eylül University
In Partial Fulfillment of the Requirements for the Degree of Master of Science in Civil Engineering, Construction Materials Program

by
Houman VAHEDI

October, 2019
İZMİR

M.Sc THESIS EXAMINATION RESULT FORM

We have read the thesis entitled "**INVESTIGATION OF EFFECT OF COATING TYPE ON CORROSION PERFORMANCE OF REINFORCEMENT BARS**" completed by **HOUMAN VAHEDI** under supervision of **ASSOC. PROF. DR. HÜSEYIN YİĞİTER** and we certify that in our opinion it is fully adequate, in scope and in quality, as a thesis for the degree of Master of Science.

Assoc. Prof. Dr. Hüseyin YİĞİTER

Supervisor

Prof. Dr. Halit YAZICI

(Jury Member)

Doç. Dr. Ali Haydar ÖZTÜRK

(Jury Member)

Prof. Dr. Kadriye ERTEKİN

Director

Graduate School of Natural and Applied Sciences

ACKNOWLEDGEMENT

Foremost, I would like to express my deepest gratitude and appreciation to my dear supervisor Assoc. Prof. Hüseyin YİĞİTER for his valuable support and guidance throughout my research, the preparation of this research would not have been possible without his continuous support and insightful comments.

I would like to acknowledge Dokuz Eylül University, Department of Civil Engineering, SARGIN Prefabrik A.Ş. and BURSA Cement Company for their material support.

My profound appreciation is extended to everyone who is directly and indirectly associated with my study and has made my research possible.

Finally, I would like to thank my dear family: my amazing wife who has always been with me for the rest of my life Beyda SARGIN. My dear mother Sepideh BANISAEID, my dear brother Houtan VAHEDI and my dear sisters Sara and Sayeh AHADI for their unconditional love and support throughout my life.

Houman VAHEDI

INVESTIGATION OF EFFECT OF COATING TYPE ON CORROSION PERFORMANCE OF REINFORCEMENT BARS

ABSTRACT

In terms of concrete or pre-stressed concrete structures, steels are fixed into the concrete matrix alongside the service life of the structure. In fact, the true designed, impermeable, high quality concrete with sufficient thickness, makes steel reinforcement, which is covered by a special mineral coating chemically and physically protected from corrosion. Today, one of the most detrimental factors in assigning service life of concrete structures is corrosion. Corrosion of steel reinforcement causes a cross-sectional degradation in rebar structure and results in the reduction of ductility of the structural element. In this study, an alternative method to protect reinforcement bars from corrosion hazards in terms of inhibitors and rebar coating usage will be discussed. Mineral coating experiments on iron were performed. Three types of mineral coating were applied by shotcrete method on rebar, these materials are ground granulated blast furnace GGBS (25 percent and 50 percent), silica fume S.F are named as K2-K3-K1. Also, inhibitaion effect of dipotassium hydrogen phosphate on the reinforcement corrosion was investigated in experimental program. The aim of this study is to reduce the deterioration process of reinforcement in structures built on the coasts of the sea and to extend the service life of the reinforced concrete elements in terms of corrosion. The result is a reduction in the corrosion rate, depending on the type of mineral coatings. The use of inhibitors, in the concrete or mortar disrupted the concrete and mortar structure. However, the cure with additive sprayed on the steel bars showed resulted in a delay in corrosion onset.

Keywords: Cement based coating, corrosion inhibitor, electrochemical corrosion measurement

KAPLAMA TİPİNİN BETONARME DONATISI KOROZYON PERFORMANSINA ETKİSİNİN ARAŞTIRILMASI

ÖZ

Beton veya öngermeli beton yapılar açısından, çelikler yapının hizmet ömrü boyunca beton matrisine gömülü kalır. Gerçekte, yeterli kalınlığa sahip doğru tasarlanmış, geçirimsiz, yüksek kaliteli beton, kimyasal ve fiziksel olarak donatıyı korozyona karşı korumaktadır. Günümüzde beton yapıların hizmet ömrünü belirlenmezsine en önemli faktörlerden biri korozyondur. Çelik donatı korozyonu, donatı yapısında kesitsel bir azalmaya neden olur ve yapısal elemanın sünekliği azalmasına neden olur. Bu çalışmada, donatı çubuklarını korozyon tehlikelerinden koruyucu ve önleyici bir kaplama kullanımı olarak alternatif bir yöntem incelenmiştir. Donatı üzerinde çimento esaslı mineral kaplama uygulama yapılmıştır. Kaplama çimento ile birlikte farklı oranlarda öğütülmüş yüksek fırın cürufu, silis dumanı kullanılmıştır. Ayrıca çimento harcı ile hazırlanan donatı örneklerde inhibitör kullanımın etkileri incelenmiştir. Bu çalışmanın amacı, deniz kıyılarında inşa edilen yapılarda donatının korozyon süresini yavaşlatmak ve betonarme elemanların korozyon ömrünü uzatmaktır. Sonuçta, mineral kaplamaların tipine bağlı olarak korozyon oranında bir azalma tespit edilmiştir. Beton veya harçta kullanılan inhibitör, beton ve harç yapısını bozmuştur. Bununla birlikte, yalın donatıların inhibitör içeren agresif sıvılara maruz kaldığında korozyon sürecinin yavaşladığı tespit edilmiştir.

Anahtar Kelimeler: Çimento esaslı kaplama, korozyon önleyici, elektrokimyasal korozyon ölçümü

CONTENTS

Page

LIST OF FIGURES

Page

LIST OF TABLES

Page

CHAPTER ONE
INTRODUCTION

Corrosion can be described as the irreversible destruction of a metal via electrochemical or chemical reaction with its surrounding atmosphere. Four factors required for a corrosion process to take place are an anode, a cathode, an electrolyte, and a metallic path. The natural process of corrosion cannot be inhibited however; intervening with the correct measures can control it. Without intervention, corrosion proceeds and becomes destructive (Pohlman, n.d.).

Depending on the type of material, the environment the material is located and the length of exposure time to that environment, corrosion can take many forms. Some of the more relevant forms of corrosion are defined below.

1.1 Galvanic Corrosion

Galvanic corrosion occurs when different types of metals join together in a medium with electrolytes present for example; seawater.

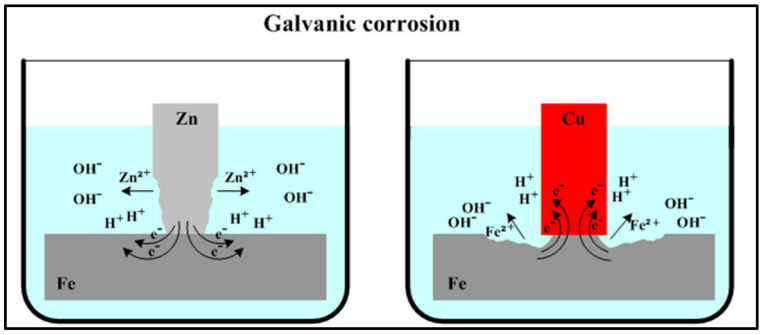

Figure 1.1 The Galvanic corrosion with joint of metals (Kopeliovich, n.d.)

1.2 Pitting Corrosion

Random destruction of a restricted section of a metal's surface can result in holes that have larger depth than width, this phenomenon is caused by Pitting corrosion.

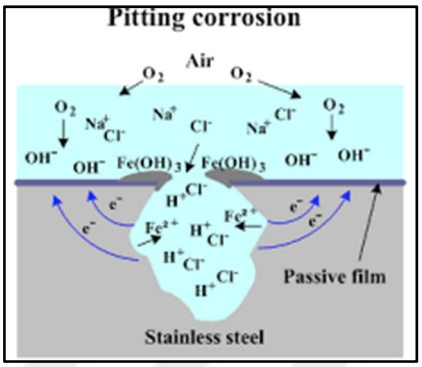

Figure 1.2 Pitting corrosion small holes in metals (Kopeliovich, n.d.)

1.3 Stress Corrosion Cracking

Stress corrosion cracking (SCC) is a form of complex corrosion occurring when tensile stress effect (a stretch or bend in a material causing it to pull apart from two sides) is combined with a corrosive environment to form dry, brittle cracks.

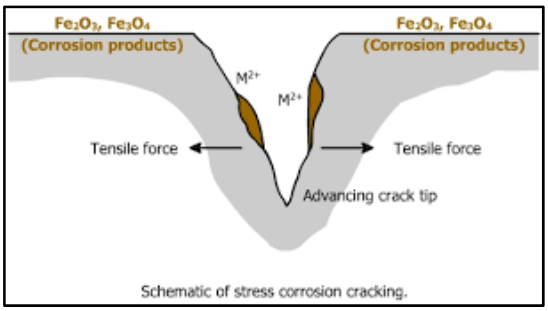

Figure 1.3 The corrosion of metals in stressed (Kopeliovich, n.d.)

1.4 Crevice Corrosion

Crevice corrosion or concentration cell corrosion is a type of corrosion occurring when a corrosive liquid gets trapped in a small narrow gap between metals, or metals and nonmetals.

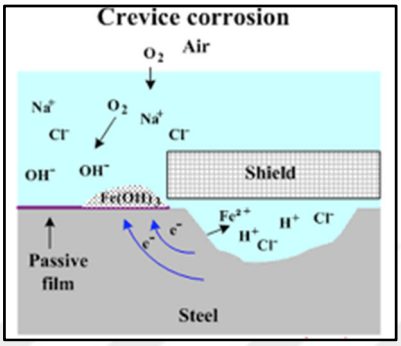

Figure 1.4 The crevice corrosion, corrosion in confined spaces where the working fluid has limited access to the environment (Kopeliovich, n.d.)

1.5 Filiform Corrosion

Another form of concentration cell corrosion is called filiform corrosion which occurs on metallic surfaces coated with a thin organic film. Typically, the surface must be somewhat acidic and the relative humidity in the environment must be 65 to 90 percent. Defected surface protective coatings are more vulnerable to this form of corrosion.

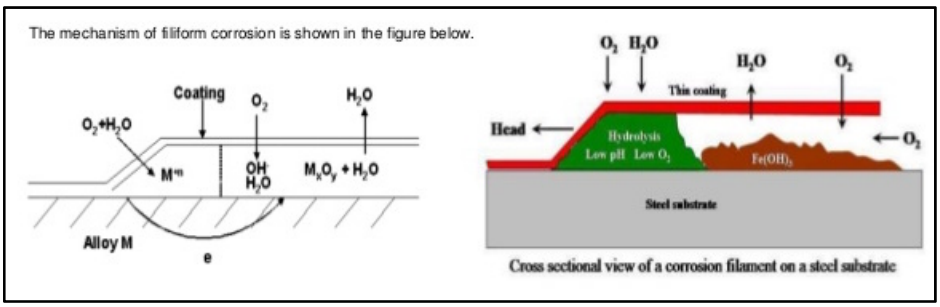

Figure 1.5 The filiform corrosion a special form of corrosion that occurs under thin coatings in the form of filaments like thread (Kopeliovich, n.d.)

1.6 Erosion Corrosion

Erosion-corrosion or flow-assisted corrosion, is an accelerated type of corrosion occurring by the movement of corrosive liquid against a metal surface, leading to its degradation.

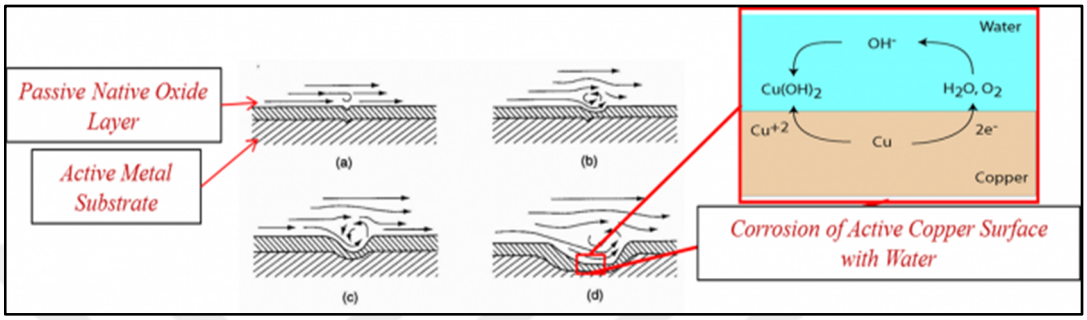

Figure 1.6 The erosion corrosion an acceleration in the rate of corrosion attack on metal due to the proportional movement of an abrasive fluid and a metal surface (Kopeliovich, n.d.)

1.7 Corrosion of Rebar in Concrete

In aqueous media the mechanism of corrosion has an electrochemical nature, meaning that metal oxidation reaction on a region of metal is neutralized by a reduction reaction on another section of the metallic surface. This will result in the polarization and formation of anode and cathode zones. A highly alkaline solution found in the electrolyte zone of concrete, naturally protects the steel embedded in it. This solution is saturated in the reaction product of complex calcium silicate compounds of cement, Ca (OH) 2 and it is a mixture of potassium hydroxide and sodium hydroxide with 12.6-14 pH. Furthermore, steel is also protected by concrete cover. Chloride Presence and Carbonation are classified as the two main reasons of electrochemical corrosion (see Figure 1.7). Although chloride causes a localized attack, carbonation makes a more generalized corrosion. The existence of rust on steel bars respectively with presence of cracks can cause of this corrosion. The cracks due to stress corrosion can also be seen in Figure 1.7, this type of corrosion develops in pre-stressed wires which have been exposed to severe destructive conditions.

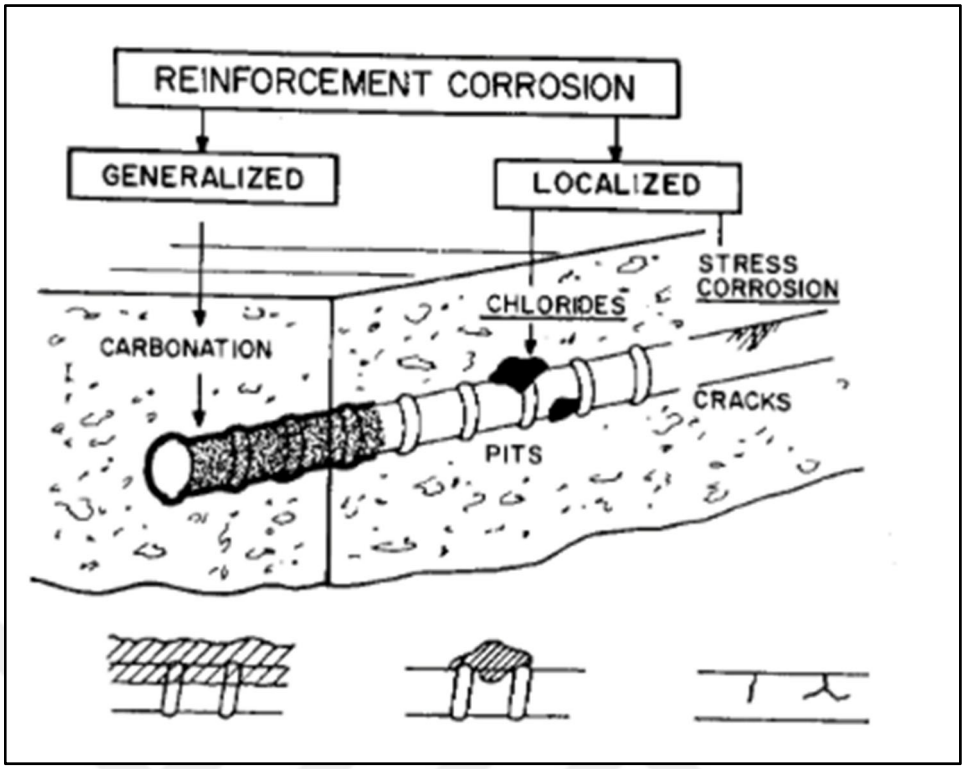

Figure 1.7 Types of reinforced corrosion in concrete (Kopeliovich, n.d.)

1.8 Type Of Corrosion In Concrete

1.8.1 Atmospheric Corrosion

Reaction of steel surface material with the atmosphere surrounding it can lead to destruction and deterioration of the steel and its necessary properties, this phenomenon is called Atmospheric corrosion. Below is the reaction of iron with oxygen and water:

$$Fe + 1/2O_2 + H_2O \longrightarrow Fe(OH)_2 \qquad (1.1)$$

$$Fe(OH)_2 \longrightarrow FeO + H_2O$$

1.8.2 Electrolytic Corrosion

An external source of electromotive force (EMF) can cause an electrical current flow between two metals causing continuous corrosion between two metallic surfaces, this accelerated process is called electrolytic corrosion (see Figure 1.8).

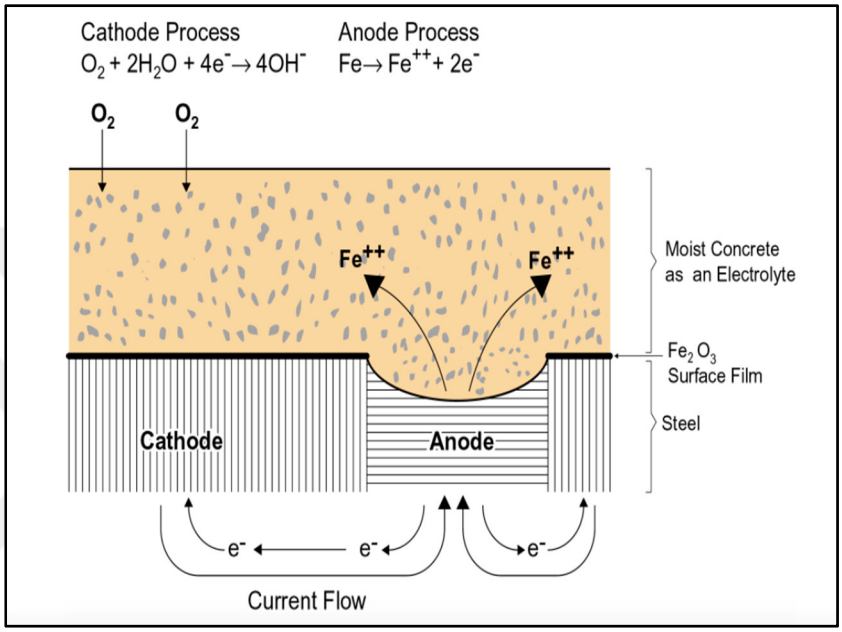

Figure 1.8 Ionization of reinforcement in concrete (Smith, 2007)

Anode process: Ionization of steel by loss of electrons

$$\mathbf{Fe \Rightarrow Fe^{2+} + 2e^-} \qquad (1.2)$$

Cathode process: Combination of excess electrons in steel

$$\mathbf{STEEL + H_2O + O_2\ FORMS\ 2(OH) - 2e- + \tfrac{1}{2}O_2 + H_2O \Rightarrow 2(OH)} \qquad (1.3)$$

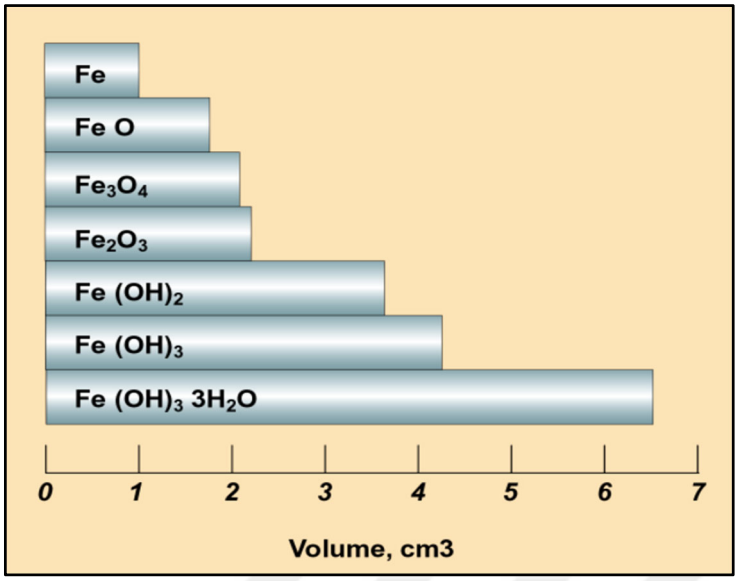

Figure 1.9 Volume change of various corrosion products (Smith, 2007)

1.8.3 Chloride Corrosion

The presence of chloride ions in concrete is not common. Most frequently, the presence of chlorides in concrete are due to usage of deicing salts or placing the structure in marine environments. Chlorides penetrate by diffusion in ingrown zones or in fully saturated concrete and them cause local disruptions.

Different factors affect the chloride threshold including:

- The availability of oxygen (corrosion potential when arriving the chlorides).
- Cement type: blending materials, fineness, amount of gypsum, etc.
- Moisture content and variation.
- Porosity belong to water cement ratio
- Porosity belong to compacting and placement
- Steel bars type and surface properties

$$Fe^{3+} + 3Cl^{-} \longrightarrow FeCl_3$$

$$FeCl_3 + 3(OH)^{-} \longrightarrow Fe(OH)_3 + 3Cl^{-} \quad (1.4)$$

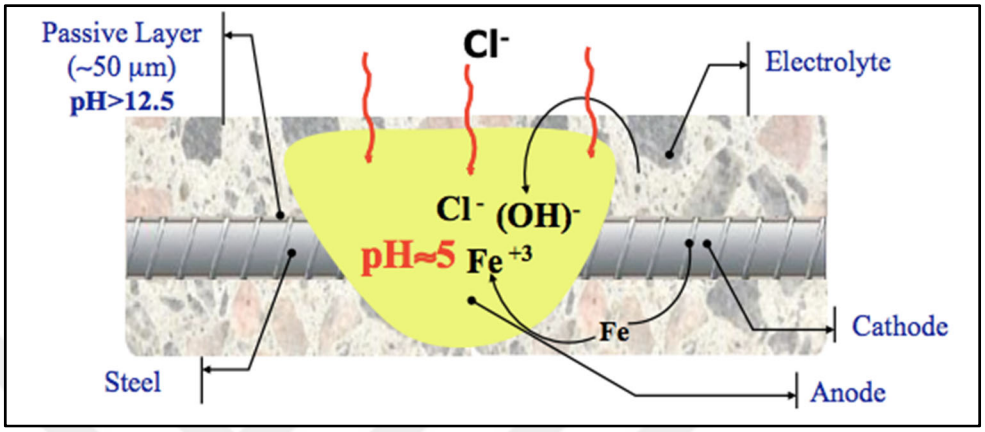

Figure 1.10 Chloride corrosion mechanism of reinforcement bars in concrete (Smith, 2007)

1.8.4 Contact Corrosion

When two different metals contact with each other, the metal, which is at upper levels of electromotive series of electromotive table means, is more stable than the other one and not oxide.

$$\text{Two different metals (in contact)} + H_2O + O_2 \longrightarrow \text{Galvanic Battery}$$

In this type of corrosion, an anodic metal loses an electron.

1.9 Service Life Of Structural Elements

In the case of reinforcement corrosion, the service life depends on humidity and another factor that reliance before, the simplest and illustrative model for describe service life shown in Figure 1.11.

An initiation period; the time, it takes the chloride or carbonation front to reach the rebar and to pass the steel from the beginning of the erection. Furthermore, a spreading time from steel passivation to a certain level of unacceptable destruction.

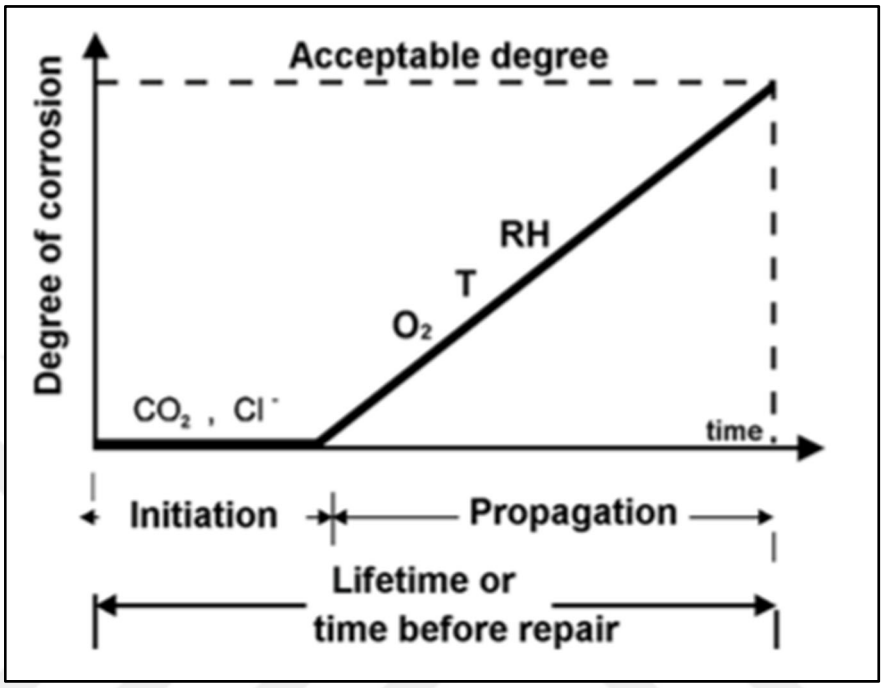

Figure 1.11 Schematic of corrosion degree (T is temperature, RH is relative humidity) (Smith, 2007)

1.10 Effect Of Corrosion On Structure

The corroding process in non-prestressed reinforcements causes a sectional decrease allowing iron oxides (rust) to have a greater volume than the original steel initiating an internal stress in concrete which may result in cracks or spalling of its cover. The structure ductility can be affected by corrosion, as it can decrease the steel prolongation. Nevertheless, Corrosion of steel bar in concrete composite can affect the mechanism of structure due to production of crack through stress of swelling of corroded steel.

The following three factors are direct results of corrosion that cause a decrease in structural mechanism:

- Corrosion caused reductions of rebar section
- Reduction of bond strength
- Cracking or spalling of cover causing loss of concrete integrity

1.11 The Effect Of Environment In The Corrosion Process

When the concrete starts aging in a specific environment, the reinforcement corrosion starts to take place causing a decrease in concrete strength. The moisture content of the concrete is the main environmental parameter that depends on humidity and external temperature. This moisture controls the CO_2 and O_2 diffusion. The carbonation gets delayed when the material is water saturated and access of O_2 gets limited. On the contrary, chloride diffuses quicker when the material is saturated. Electrical resistivity (porosity) is affected no matter the corrosion process.

The effect of moisture is not homogeneous, in fact it is a gradient produced from the concrete surface leading to the interior. Temperature and rebar position (cover depth) can also influence the corrosion process. Acceleration or retardation of the reaction can be produced. The oxygen of the pore solution can be eliminated when the temperature levels increase, and evaporation occurs. Therefore, although corrosion is caused by higher temperatures, it can be neutralized by evaporation. Lowering the temperature has adverse effects.

Relative humidity and temperature cannot be directly quantified, and the humidity of the concrete depends on the external relative humidity and rain. Raining can influence the saturation degree of the concrete intensely. Therefore, the degree of saturation is a better parameter to resistance and corrosion values. The exposure of concrete to a certain outdoors conditions will cause a saturation degree specific for that humidity and temperature allowing parallel changes in the concrete moisture content.

Accelerated corrosion test took place in this study. In the applications, construction irons were coated by spraying method at the specified dosages, and the coatings were cast in concrete in special molds (method specified as lollipop recipe) with 2 cm cover.

After 7 days of curing, the samples were left to test with rapid corrosion method. The Rapid Corrosion method was done with Gamry interface 1000 potentiostat device that was used for corrosion measurement. electrolyt medium in the system, sodium chloride and 3.5% NaCl solution was prepared using pure water in an ambient temperature of 18-20°C. The rapid corrosion test, open circuit potential was measured at 3600 seconds. Potentiodynamic and Tafel results were evaluated for the samples measured between -0.2v and 0.2v, and measurement speed 0.2mv/s, and density 7.87g / cm^3. 1 v application for potetiostatic results were measured up to 72000 seconds. The aim of this study was to increase the life of the structure by coating methods. With the coating method, we observed that iron was exposed to corrosion late.

CHAPTER TWO
LITERATURES

2.1 Mechanisms Of Corrosion Induced Cracks In Concrete At Meso-Scales And Macro-Scales

In the paper by Ohtsu and Uddin, the initiation of corrosion in reinforcement is followed; cracks can be generated in concrete by expansion of corrosion products. They used acoustic emission techniques for detecting the micro cracks caused by corrosion.

They placed rebar in concrete, and then embedded in to the NaCl water to make salty surroundings. The cracking caused by expansion of corrosion merchandise on the surface of rebar, takes place in exceptionally long-term scales. Concrete specimens of dimensions (250x250x100) mm with hole of 30mm diameter had been examined (Ohtsu, 2008).

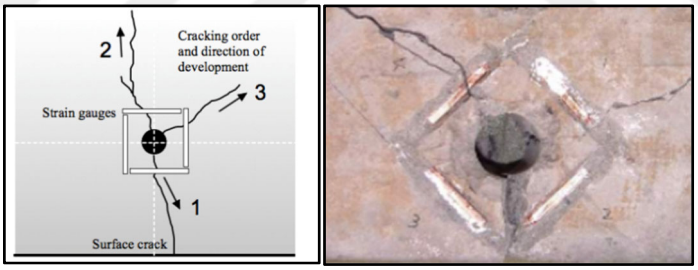

Figure 2.1 Cracking and direction of development of corrosion (Uddin, 2008)

The results of this experiment found a floor crack and two diagonal cracks in specimens which reveal that diagonal cracks are generated following the surface cracks. Those definitely reveal that diagonal cracks are inherently generated following the surface crack. Within the experiments described, the era of corrosion-caused cracks become simulated with the aid of appearing expansion tests on concrete specimens containing a hole.

2.2 Protection Of Steel Embedded In Chloride-Containing Concrete By Means Of Inhibitors

In this paper, Gonzalez, Ramirez and Bautista try inhibitor to protect iron from corrosion. They used $NaNO_2$ to see if it can counter the corrosive effect of chloride on reinforcement that are embedded in mortar blended with synthetic sea water. They used mortar specimens with 2x5x8 cm dimensions with each of them having an 8 mm reinforcement steel rods. The steel rods were positioned in symmetry and were used as operational electrodes. Sufficient protection was observed by using 1% nitrite in 1 to 720 days shown in Figure 2.2

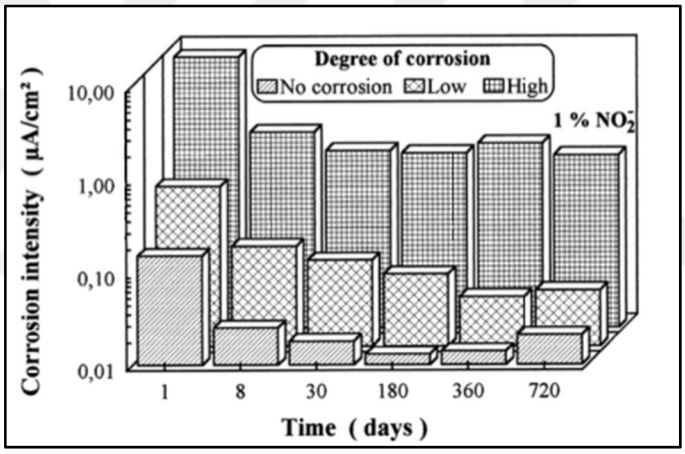

Figure 2.2 Corrosion intensity (Gonzalez, 1996)

Evaluation of preliminary and expected i_{corr} values of pre-rusted steel electrodes embedded in Mortar containing 1% NO_2^- after exposures for 1, 8, 30, 180, 360, and 720 days. When compared to other inhibitors, Nitrite showed 0 to 2% higher chloride surroundings than others shown in Figure 2.3.

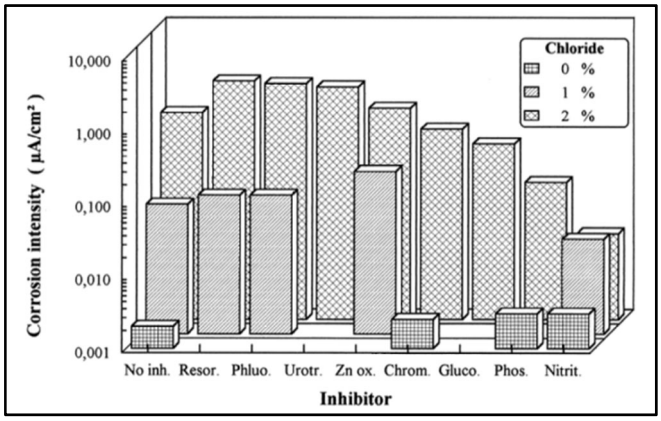

Figure 2.3 corrosion intensity of inhibitors (Gonzalez, 1996)

When adding 2% $NaNO_2$ to the mortar the possibility of corrosion in reinforcements embedded on concrete mixed with seawater is effectively countered. Some of the dissolved nitrite inside the aqueous part of the concrete pores are filtered under immersion situations. This would hold up the hypothesis that a stronger concrete system submerged in salty water could not be completely covered. The length of powerfulness is proportional to concrete quality.

2.3 Effect Of Pumice On Steel Corrosion

In this study Binici, Zengin, Zengin & Yasarer (2008) investigated the effect of pumice used as coating on restriction of corrosion, they provided pumice from pyroclastic exposure in from regions of Turkey. 5% and 10% $NaSO_4$ solutions were used to uncover specimens. The measurements of checking corrosion was done with evaluating mass losses of steels and the compressive strengths of concrete were also measured. The results shows that specimens with growing layers of pumice coating had an improvement in these two variables and their corrosion rate was lower than the controls. A high association was seen between reinforcement corrosion and types of pumice coating. By increasing the amounts of SiO_2 the corrosion ratio reduced. The experimental study used as two method, the first method was mass losses of the concrete specimens and the steel bar, the second method measurement of compressive strengths. The dimension of the concrete specimens used were 100x100x100 mm and the resistance of reinforcement steel to corrosion attack was studied. The specimens

were either coated or uncoated. The specimens were coated with one layer and 2 layers and they were names as Van pumice (VP), Kayseri pumice (KP), Nevsehir pumice (NP) and Osmaniye pumice (OP) (Binici, 2008).

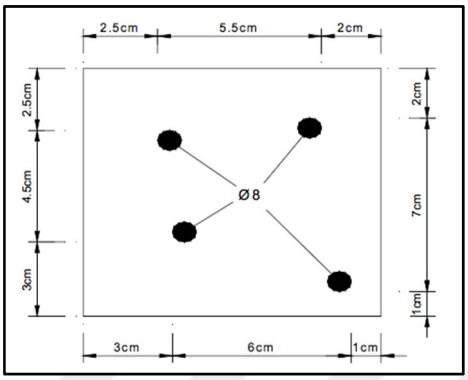

Figure 2.4 Rebar coverd mould sample (Hanife, 2008)

The rebar corrosion was evaluated in two approaches: rebar surfaces of certain masses were fixed in moulds and were covered with pumice coated which are dyed basaltic pumice coatings. Both coated and non-coated rebars which were used as controls were fixed in the $NaSO_4$ solutions. The concrete specimens' surfaces lined with a single layer of PUMCO were represented as VP1, NP1, KP1 and OP1 and those with double layers as VP2, KP2, NP2 and OP2. To determine the percentage of corrosion and the effect of exposure of the steels, mass losses were determined in RS bars and modifications in pH values have been recorded for monthly intervals. There was almost no deterioration of the concrete surface when it was coated with PUMCO, although the PUMCO coating itself had deterioration. The corrosion of the concrete was much lesser in PUMCO coated than in the uncoated control specimens and there was no deterioration of the central core of the concrete, only very small parts of the exterior surface. The results showed that the coating itself displayed resistance towards $NaSO_4$ attack. The results of the sulphate resistance assessments performed on the control sample and the single layer PUMCO coated specimens in Na_2SO_4 solutions are depicted in Figure 2.4.

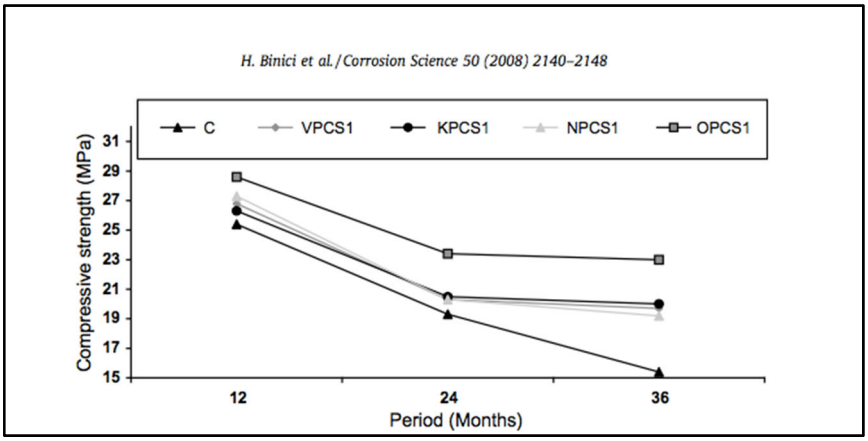

Figure 2.5 Compresive strength (Binici, 2008)

Mass lost against time is shown in Figure 2.6. For concrete specimens. After 12 months under sulphate solution, the mass loss for control specimens were 4% while for PUMCO specimens was only 1%. After 24 months of exposure, the numbers increased to 10% for control and 5% for PUMCO specimens, concluding that coating the concrete demonstrates a better behavior against Na_2SO_4 attacks, in both long and short terms.

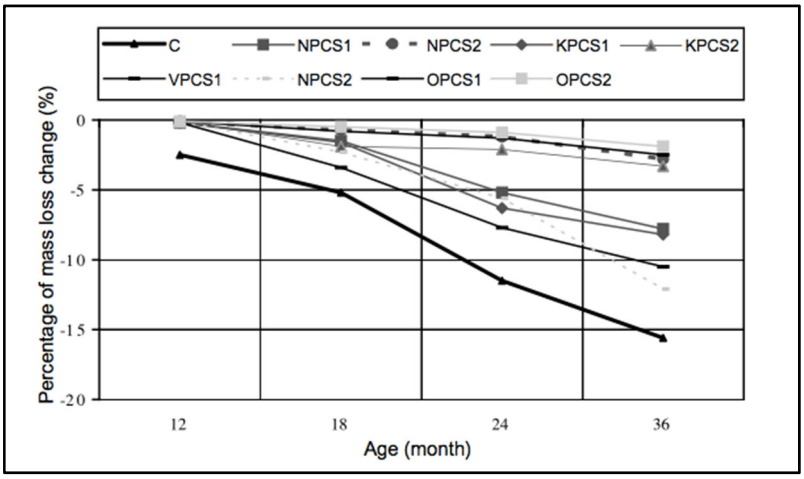

Figure 2.6 Mass loss of coating sample (Binici, 2008)

In conclusion, when increasing the coating layer of the concrete, the compressive strength enhanced clearly. Reinforcement Steel's corrosion resistance increased in OPRC specimens. In comparison with uncoated control specimens, PUMCO provided

an improved resistance for corrosion. The corrosion rate of control specimens was a lot higher than the pumice coated specimens. Therefore, indicating that as increasing the coating, the resistance for corrosion also increased.

2.4 Reinforcement Concrete Corrosion On Different Curing

Steel reinforcement corrosion, electrical resistivity, and compressive strength of concretes were investigated in this study. By using plain and four different blended Portland cements, concretes with different cement contents and water were prepared and three type of curing were applied on specimens. By using an accelerated impressed voltage setup, the impact of using plain or blended cements on the resistance of concrete against harm caused by corrosion of the embedded reinforcement. The electrodes were placed on the concrete surface to measure the resistance of the cover concrete. The compressive energy, electrical resistivity, and corrosion resistance of the concretes were decided at multiple ages up to 180 days (Guneyisi, Gesoglu, Ozturan & Ozbay, 2009).

In this experiment 5 different cements were used. The dry ingredients were first mixed for one minute and then water was added, and it was mixed for 3 more minutes. The dimensions for cubes and cylinders were 150x150x150 mm and 100x200 mm, respectively. Cubic and cylinder specimens were prepared for compressive strength and electrical resistivity, respectivly. The accelerated corrosion test was performed using 100x200 mm reinforced concrete cylinders in which a 16mm diameter steel bar was fixed centrally. The steel bar was embedded into the concrete cylinder such that its quit changed into at least 30mm from the bottom of the cylinder, and it was lined with epoxy on the exit from the concrete cylinder in order to remove crevice corrosion at those locations (Guneyisi et al., 2009).

As it shows in Figure 2.7, the compressive strengths were subjected for concretes specimens for evaluating the strength for 28 days, 90 days and 180 days. Depending on the age, w/c ratio, and curing conditions that were being tested, the strength values are ranged between 20 to 70 MPa.

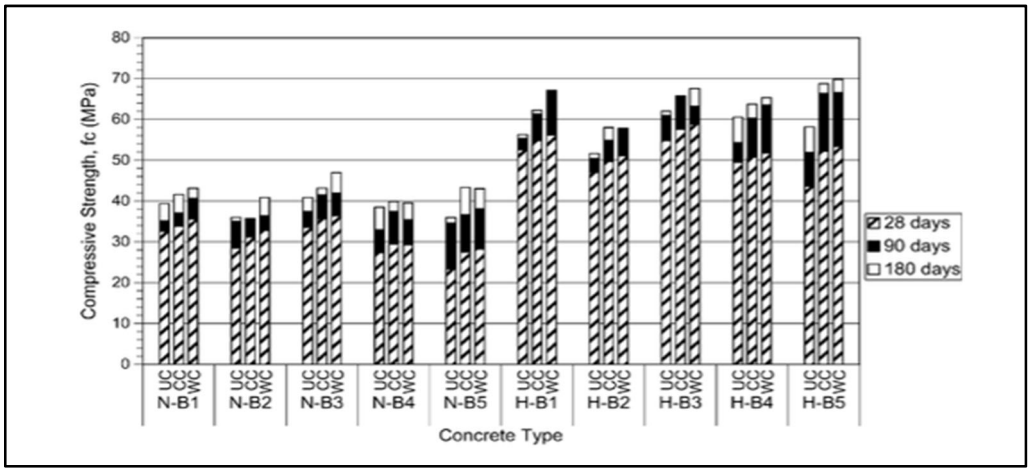

Figure 2.7 Compressive strength concretes with different type of curing conditions (Guneyisi, et al., 2009)

As it shows in Figure 2.8, Effect of curing on compressive strength of 28 days and 180 days of different concrete specimens. Uncontrolled curing caused decreased 28 and 180-day strengths in both concrete types. It was seen that specimens cured with controlled and wet curing had 5% equality in compressive strength in both concrete types shown in Figure 2.9.

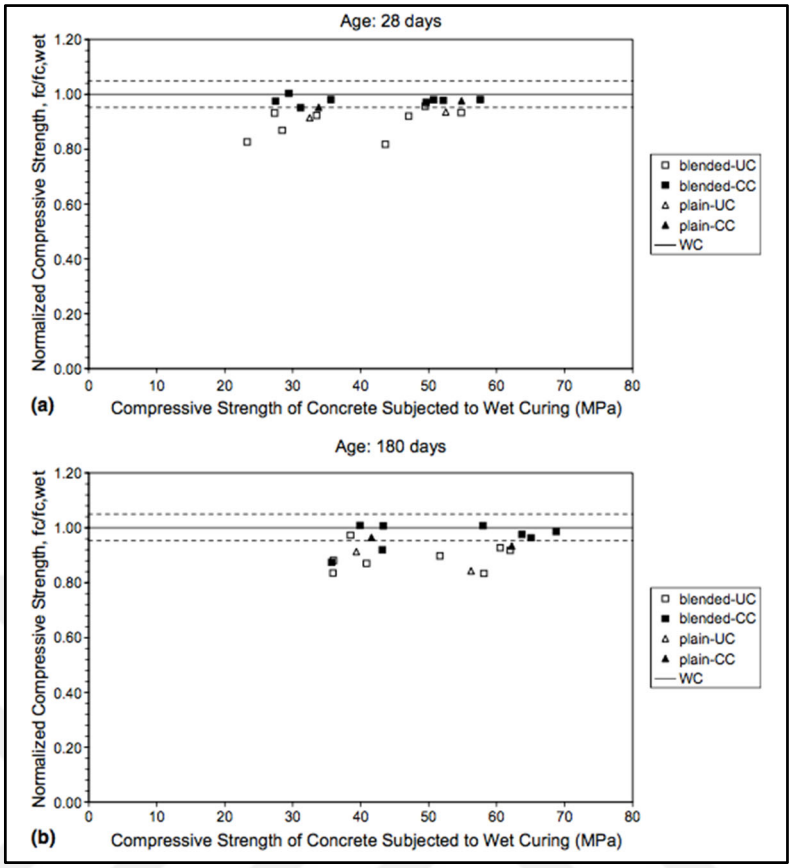

Figure 2.8 Electrical resistivity concrete specimens due to different type of curing conditions (Guneyisi, et al., 2009)

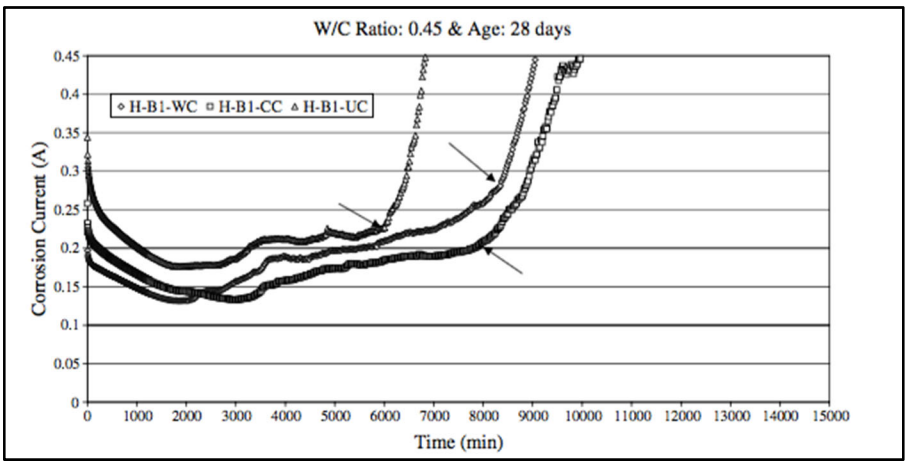

Figure 2.9 Time and typical corrosion current curve over 28 days of test age for concretes made with Portland cement under different curing conditions (Guneyisi et al., 2009)

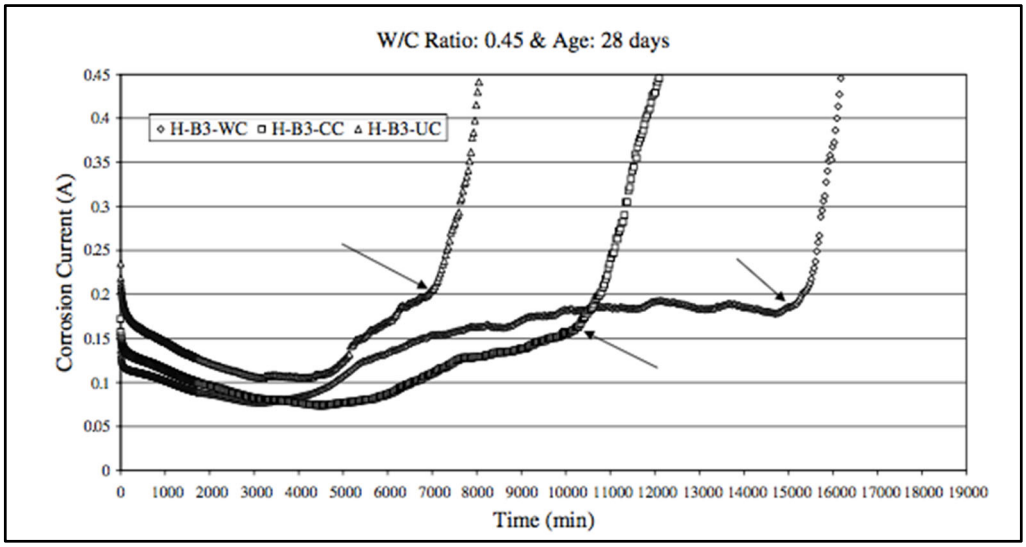

Figure 2.10 Typical curve versus time of corrosion current at 28 days of test age for concretes made with Portland composite cement under different curing conditions (Guneyisi et al., 2009)

Figure 2.11 Specimens after corrosion test (Guneyisi, et al., 2009)

Consequently, different cement, water-cement ratio, age and curing type had a tremendous outcome on each electricity and durability of concrete. Both two type of cement concrete specimens exposed to air curing showed decrease overall performance in résistance of corrosion and strength in comparison to managed and wet curing processes. Figure 2.10, Figure 2.11 Managed hardening furnished a median compressive power of 5% of these received inside the moist hardening procedure for each concrete sort. However, the strength of the flat and blended cement concrete

samples underneath the uncontrolled hardening circumstance from those hardened under wet hardening via 10% and 20%, respectively. Both out of control and controlled curing processes have ended in great variations in wet curing in terms of electrical resistance. The multiplied corrosion equipment used in this take a look at become found to be an effective and easy device for assessing the robustness performance of concrete.

2.5 Effect Of Atmospheric Pollution On Steel Corrosion

The purpose of this experiment, four different reinforcing steel rebar sets, S220, S400, S500 Tempcore and S550s Vanadus were tested by exposing them to Greek atmosphere before installing them into concrete. The capacity of the different sets of steel were measured using microscopic techniques and by measuring the corrosion rates. Specifically, the effect of corrosion products of the steel reinforcement on the strength of bonds between steel bars and concrete was studied while the cement hydration was processing. The morphology of the corrosion product cements and rust strains where studied using microscopical techniques and by visual observations before embedment into the concrete.

The results of the experiment showed that the most resistance to the atmospheric corrosion problems was S220 type steel reinforcement, these results were observed while the S500 Tempcore reinforcing steels showed the least resistance to corrosion. The results showed that the weathering and bond strength between the concrete and steel bars are negatively associated and as the weathering increased form 45 days to 122 days, the bond strength decreased, based on the observations by ESEM, this was because of the accumulation of rust on the steel bars and formation of thick layers on them.

The aforementioned still bars were in cylindrical shape (100mm long and 12mm diameter), the specimen were tested for three months in Patissia corrosion station, Athens. After three months the weight loss of the steel bars was measured, and the corrosion rate was accordingly calculated by using the following equation (Batis & Rakanta, 2005).

$$\text{Corrosion rate (μm/year)} \qquad 8.768.76 \times 10^{7} \frac{W}{A \times T \times D} \tag{2.1}$$

Corrosion rates of the test specimens are summarized in Figure 2.12.

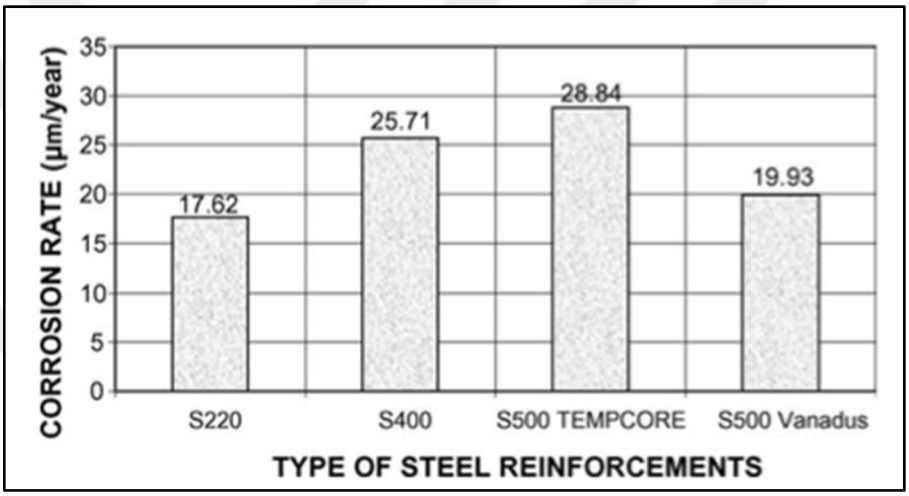

Figure 2.12 Type of steel reinforcement corrosion rate (Batis & Rakanta, 2005)

Corrosion rates of the test specimens are summarized in Figure 2.12. The S220 rebar's had the most thickness and the most uniform surface as shown in Figure 2.13(a). The atmospheric pollution was subjected for three months, these results were observed while S400 and S500 Tempcore rebars showed pitting under their rusted surface Figure 2.13. (b) and (c).

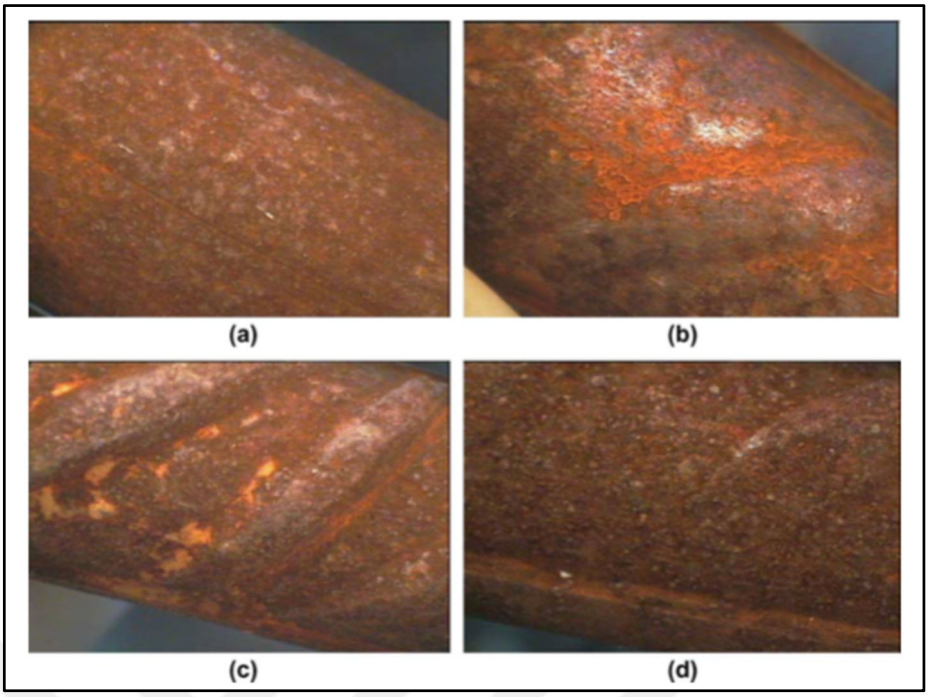

Figure 2.13 Steel surface corrosion microscopy images (Batis & Rakanta, 2005)

Commonly, through to the low adhesion bond of concrete and steel bars belong to corrosion, by increasing of rust in surface of steel the bond decrease sharply. pitting cause's decline in the ribs of rebar's (Batis & Rakanta, 2005).

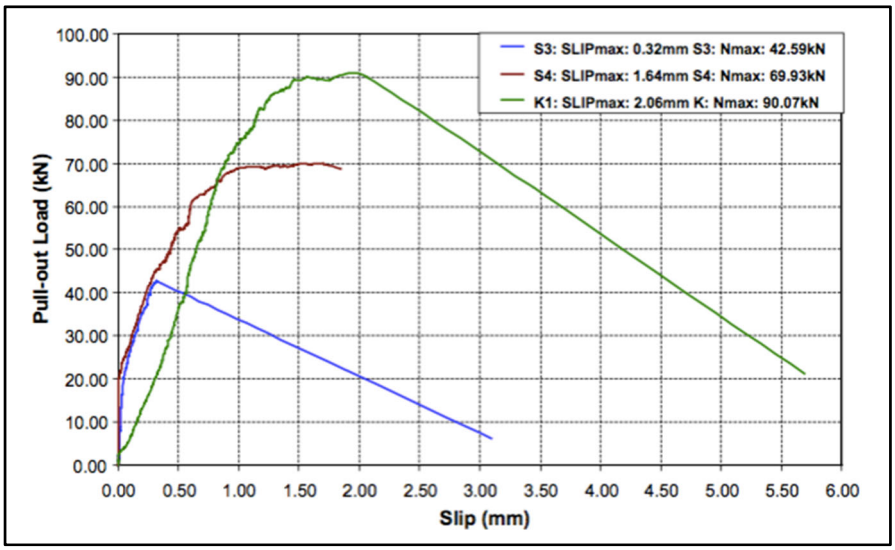

Figure 2.14 Pull-out of steel bars and concrete belong to different corrosion time (Batis & Rakanta, 2005)

The empirical results showed that the s500's tempcore metal rebar products tend to be more favorable in environmental conditions than the s500's vanadous metal rebar. The metal type s220 reinforcing metal, which exhibits as high resistance as a distance, such as atmospheric corrosion problems, has turned into metal. On the contrary, the s500s Tempcore has the lowest corrosion resistance. Among the manufacturing strategies of the 500s, only vanadium added, Figure 2.14 shows higher corrosion resistance. Steel corrosion products were transported from the steel floor of great thickness to the interior of the concrete. The iron oxides remaining on the steel floor have a porous shape, in reality there is a reality which results in the improvement of micro galvanic corrosion and consequently the increased corrosion load of the supported structure. Pre-oxidized steel rebar has shown great decreases in wire rod strength; the deterioration in the bond changed depending on the morphology and the thickness of the corrosion goods in the steel reinforcement. As stated in the ESEM observation, the bond strength between concrete and steel rebar was found to be reduced by increasing the weather from 45 days to 122 days due to the morphology and thickness of the rust layer on the steel surface.

2.6 Effect Of Inhibitors On Steel Corrosion

One of the most important investigations to can be taken into consideration on this look at is the function of phosphate inhibitor. The effect of inhibitors types on corrosion in latest years become more important. In one of study, sodium phosphate was used as an inhibitor. The inhibitor was add to the mix design. The significant result of study was the corrosion resistance capability of steel in chloride solution. Nahali, Dhouibi & Idrissi (2014) were illustrated that sodium phosphate could be used as an inhibitor in reinforcement concrete. This research done with several test methods. The corrosion resistance of steel was proven by electrochemical measurement test.

Nahali et al., (2014) were prepared cylinder specimens with embedded steel bar that have 30mm diameter and 600mm length, as is presented in Figure 2.15.

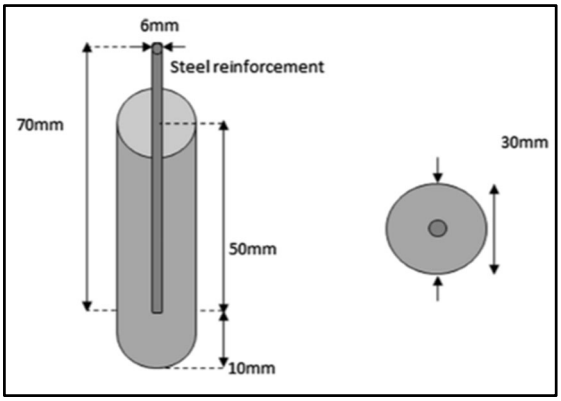

Figure 2.15 concrete casting samples (Nahali, 2014)

The prismatic specimens with 40x40x160 mm^3 dimension were cast for flexural strength test. Furthermore, the 50×50×50 mm cubic specimens were cast for compressive strength test. The effect of inhibitor was investigated on mechanical properties of the concrete. The using of inhibitor may have significant positive effect on corrosion restriction. Whereas the mechanical properties of concrete are also important. Every specimen corresponds to numerous electrochemical measurements cycle as following:

(1) Development of corrosion ability up to stabilization.
(2) E Electrochemical impedance diagram recording at Ecorr.
(3) Polarization curves plot i = f (e).
(4) Anodic polarization at imposed ability (eimposed = 1000 mV/SCE)

The first measurement collection was finished before anodic polarization (expressed as C0). The second, C1 is the primary set of measurements performed after the first anodic polarization, and C2 is the second set of measurements recorded after the second anodic polarization.

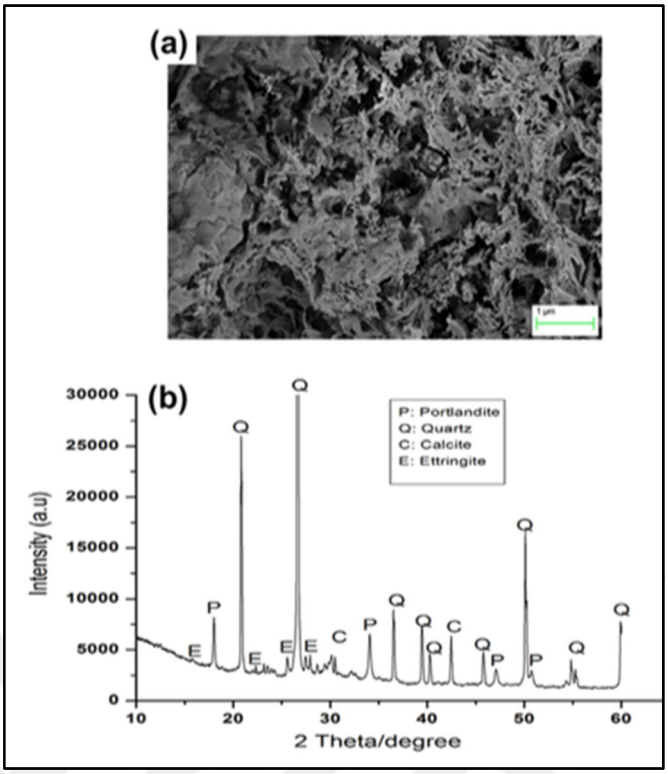

Figure 2.16 observation (a) and X-ray analysis (b) of reference samples, after 28 days of curing" (Nahali et al., 2015)

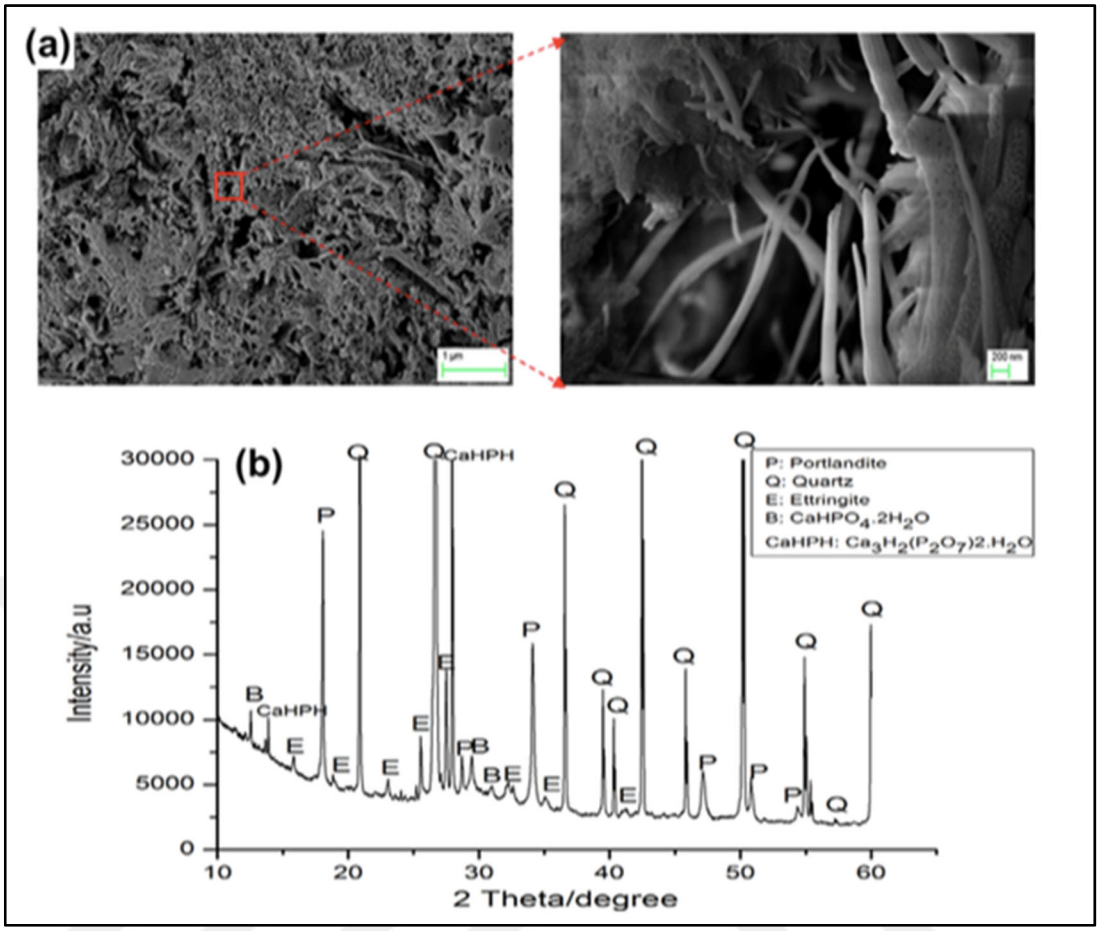

Figure 2.17 SEM survelliance (a) and X-ray displeasure analysis (b) of the sample containing 5% sodium phosphate, after 28 days of curing (Nahali et al., 2015)

As it shows in Figure 2.17, Figure 2.18 the Elasticity module for preventive and non-preventive samples during the retention time. The series increases for both samples during the first curing time and then becomes close to 39 ± 1 gpa. At the beginning of the cure, hydration reactions appear to occur normally and cause hydrate formation, ie, CSH. From 8th curing days, the hydration load becomes gradual and natural.

Crystalline salts are formed which contain calcite and phosphate and contain mainly the base compound and chloride. In addition, the elastic modulus appears to be generally less than in the case of sample without inhibitor, in the case of sample mixed with 6% $Na_3PO_4 12H_2O$. The presence of this additive in the sodium phosphate mortar seems to slow the cement hydration kinetics. He said that concrete can be

considered as prolong the placement time (Nahali et al., 2015, p.95).

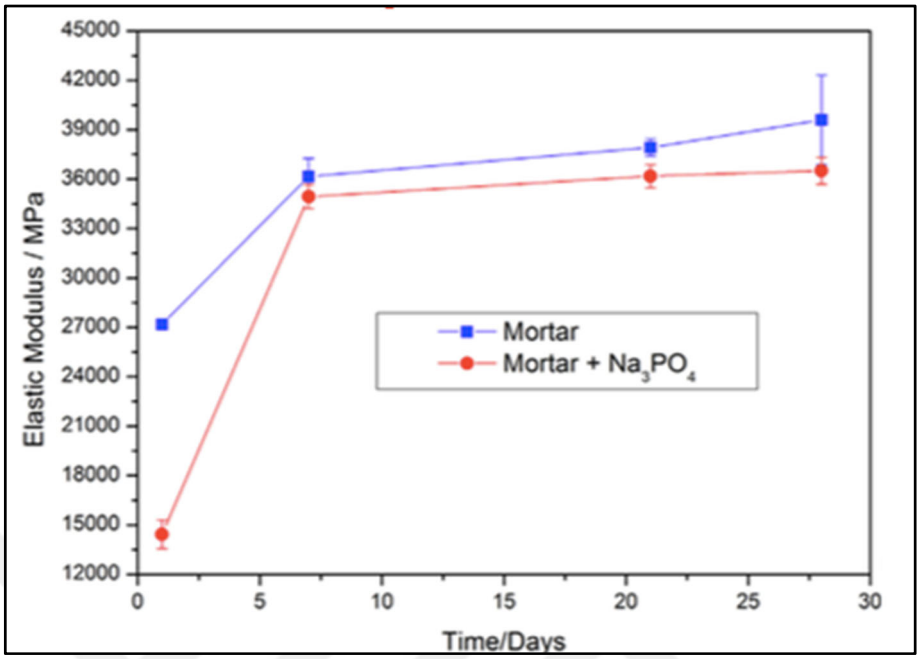

Figure 2.18 Elasticity modulus evolution (Nahali, 2001)

For each sample type, all of the cyclic polarization curves recorded during the first cycle measurement (C1) are typical in a passive country (Figure 2.19. A and b). Indeed, a passivation plateau, a low anodic current density and the absence of a hysteresis ring represent them. This behavior indicates that before any steel pattern polarization, the pre-formed passive layer on the steel surface prevents the initiation of corrosion. The evaluation of the characteristic values measured during this entire C1 cycle indicates that the reinforcement was better covered when the slurry contains Na $_3$ PO $_4$. Of course, in the passivation ability (i220mv = 0.8 ± 0.01 1 / cm2), the contemporary density of the passive layer laid is less than the reference mortar. Similarly, the pitting capacity combines re-passivation capacity, and the difference is very high (Nahali, 2015, p.95).

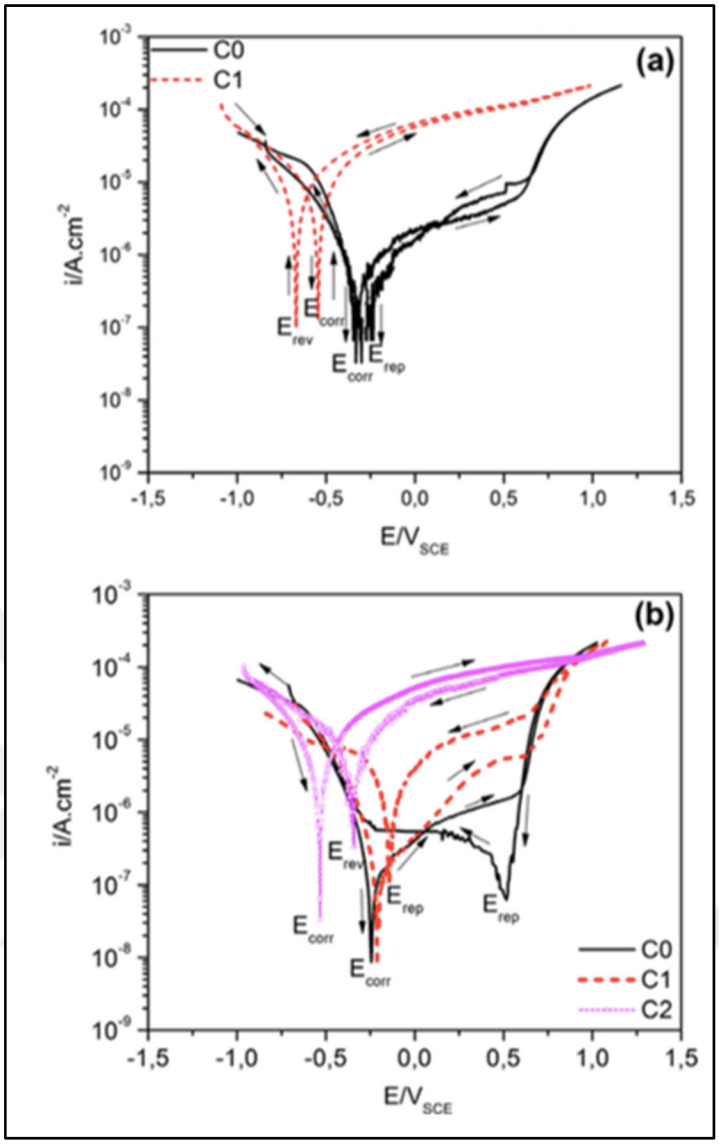

Figure 2.19 Cyclic polarization curves for hardening of reinforcements in sample samples with (a) and Na3Po4 (b) recorded during measurement of each cycle (Nahali et al., 2015, p.97)

For the control samples tested under the same conditions, the polarization chart is vividly normal. Lack of passivation and excessive corrosion innovative density characterize generalized corrosion Table 2.1 Lack of passivation plateau and excessive corrosion innovative density characterize generalized corrosion. In fact, it is seen that the chloride-containing material reaching the reinforcement base significantly exceeds the cost of steel depacivation. This causes the spread of corrosion. The shafts that undergo secondary anodic polarization (Eimp, C2 cycle) of the electrochemical behavior of the phosphorous adjuvant system are typical of an

active device. Corrosion current-day density reaches 4.9 la / cm^2. In Table 2.1, the absence of the passivation plateau and the extra corrosion innovative density characterize general corrosion. The ions of the chloride mixed in the pore response spread the iron reinforcement in the direction of the solid and this purpose prefers to passivation to begin passivation. In this case, precipitation of phosphate compounds would be insufficient to protect the steel floor against corrosion (Nahali et al., 2015, p.97).

Table 2.1 Lack of passivation plateau and excessive corrosion cutting edge density characterize general corrosion

Electrochemical parameters derived from CP tests of reference mortar exposed in 3% NaCl solution.

Mortar	Cycles	E_{corr} ± 10 (mV/SCE)	I_{corr} ± 0.1 (μA/cm^2)	I_{200mV} ± 0.1 (μA/cm^2)	E_{rep} ± 10 (mV/SCE)	I_{rep} ± 0.1 (μA/cm^2)	E_{rev} ± 10 (mV/SCE)	I_{rev} ± 0.1 (μA/cm^2)
Reference mortar	C_0	−326	0.5	2.8	−251	0.5	–	–
	C_1	−546	5.9	76.3	–	–	−669	6.2

Electrochemical parameters derived from CP tests in mortar specimens containing 5% $Na_3PO_4 \cdot 12H_2O$ exposed in 3% NaCl solution.

Mortar	Cycles	E_{corr} ± 10 (mV/SCE)	I_{corr} ± 0.1 (μA/cm^2)	I_{200mV} ± 0.1 (μA/cm^2)	E_{rep} ± 10 (mV/SCE)	I_{rep} ± 0.1 (μA/cm^2)	E_{rev} ± 10 (mV/SCE)	I_{rev} ± 0.1 (μA/cm^2)
Mortar + Na_3PO_4	C_0	−246	0.1	0.9	509	0.4	–	–
	C_1	−210	0.3	1.6	−135	2.6	–	–
	C_2	−530	4.8	75.5	–	–	−354	4.51

E imp = drift intensity excess = 1000 Mv / SCE. Chronoamperometry curves recorded at a capability equal to 1000mV / SCE over each cycle time are shown in Figure 2. It seems so:

- At any result of the cycle, the current density decreases. This is attributed to the development of a positive layer or corrosion product layer on the metallic surface.

- for the duration of each first anodic polarizations (E_{imp} in C1 and C2), the densities of the pattern containing PO inhibitor are low as compared to that located within the third cycle (C3) (Nahali et al., 2015, p.97).

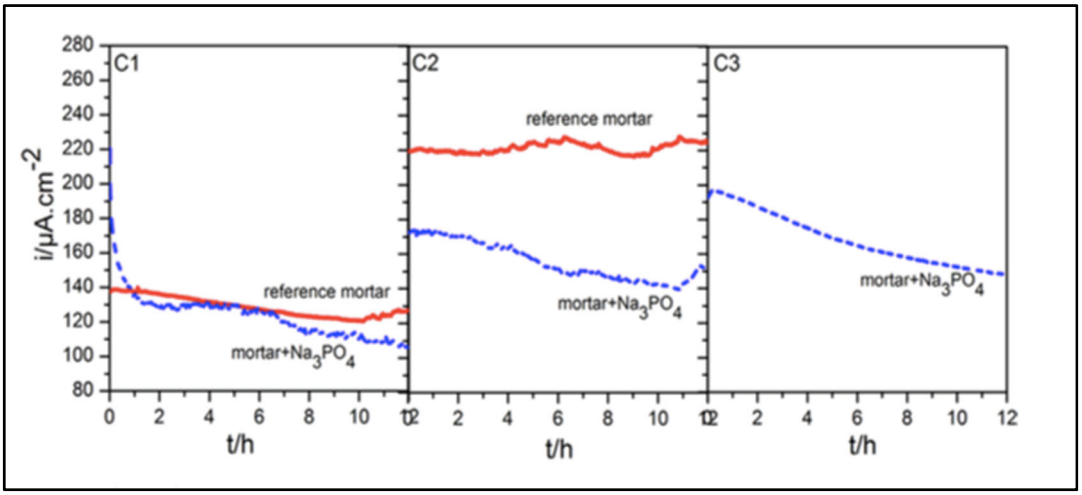

Figure 2.19 Chrono amperometry curves for reinforcing iron in mortar samples with (A) and phosphate inhibitor (b) were recorded at a potential equal to 1000 mV / SCE during each cycle. (Nahali, 2001)

The results of electrochemical tests in Figure 2.19 . Indicate that specimens that used inhibitors had a slower rate of corrosion compared to the specimens without inhibitors (Nahali et al., 2015, p.98).

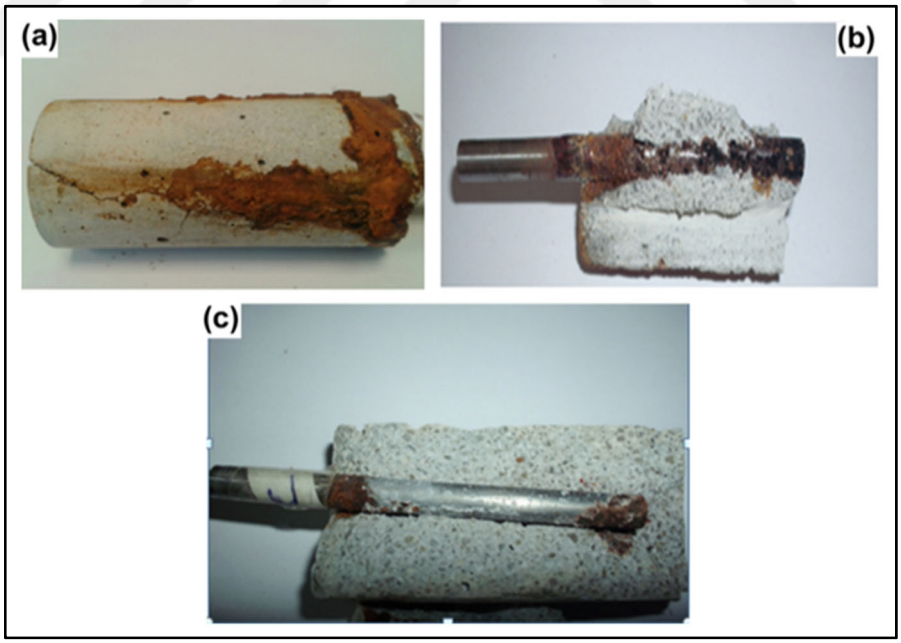

Figure 2.20 Test samples without (a) and (b) and (c) PO_4 inhibitor after corrosion (Nahali, 2001)

In conclusion, New phosphate products can be shaped when the the Na_3PO_4 inhibitor does not hydrate with cement components and cause corrosion. These products, particularly; Ca_3H_2 $(P_2O7)_2$ H_2O) and Ca_2HPO_4 $2H_2O$ block the mortar pores. Compressive strength and elasticity modules of the concrete have decreased with the disappearance of traditional cement hydrates show in Figure 2.21 (Nahali et al., 2015).

The steel is protected efficiently against the localized corrosion, when the phosphate content near the reinforcement is increased due to the passive layer that is formed on the surface of the rein. A constant compound subsuming phosphates particularly $FePO_4$, Fe_3 $(PO_4)_2$ is formed when the anodic sites of reinforcement is blocked, and chloride diffusion is restrained by the inhibitor that is presented in the concrete pore solution. It is shown that Acoustic Emission (AE) can be a useful instrument of viewing and tracking disruption of sample reinforcement by looking at the correlation between acoustic activity and polarization curves.

CHAPTER THREE
EXPERIMENTAL STUDIES

3.1 Propose

In this study, it is aimed to effectively reinforce the mechanism of action of factors affecting the degree of corrosion events in seismic zones and seashore atmospheric zone and to reveal long-term experiments. The applications were made in the laboratory environment. The basis of the experimental studies consisted of four separate sections as shown in Table 3.1 Experimental studies.

3.2 Experimental Studies

Table 3.1 Experimental studies

Section 1	Pre-trail work Concrete mix design Properties of uses materials Chemical composition of steel	Usability of the method, the initial corrosion rate values
Section 2	Studies on measures Mineral additives Cement W/C ratio	Monitoring the development of corrosion in corrosive environments
Section 3	Mineral additives dosage and cure method S.F, GGBFS Dosage (25%-50%) (Water, Salt, Air) Cure method Coating application (mineral)	Mineral additives Dosage Investigation S.F (K1) GGBS 25 (K2) GGBS 50 (K3)
Section 4	Concrete cover and Specimens Dimensions 2 cm - 70×70×300 cm	To investigate the effectiveness of protection
Section 5	Corrosion Analysis	Open circuit potential Potentiodynamic Tafel results Potetiostatic

3.2.1 Materials

The experimental program used within the framework of the electrode system with corrosion phenomena in anodic polarization method was tested. The aim of this section is to systematically test and the suitability test will be carried out method. For this purpose, reinforced concrete greatly affects the quality of concrete elements, concrete compositions were produced. The water per cement ratio 0.5, cement dosage 400 kg/m^3 were used. Corrosion measurements in concrete samples prepared for CEM-I 42.5 R type cement is used. Equally crushed limestone as aggregate in concrete mixture in the range of 0-5 mm and 5-15 mm in size were used. The chlorine content of the aggregates was determined by chemical analysis as 0.0002%.The blend details, Fine and coarse aggregate used in this study are shown in Table 3.2. The cement used was taken from the bursa concrete company. The technical specifications of the cement used as CEM-I 42.5 R were measured from the bursa concrete laboratory and delivered to us.

The properties and moisture content of the aggregates used are shown in Table 3.4.

Table 3.2 Concrete mixture

Cement(kg/m^3)	400
Water (lt/m^3)	200
0-5 mm aggregate (kg/m^3)	850
5-15 mm aggregate(kg/m^3)	885
Total (kg/m^3)	2335
Slump, cm	10
Cl content %	0.0112

Table 3.3 Chemical and physical properties of cement

(CEM I 42.5R) Chemicals analysis %	Cement
SiO_2	20.52
Al_2O_3	4.83
Fe_2O_3	4.68
CaO	63.15
MgO	1.43
Na_2O	0.22
K_2O	0.68
SO_3	2.64
Cl	0.0103
Loss on ignition	1.85
Insoluble residue	0.61
Free CaO %	1.76
Free weight	3.12
Free surface	355
ASTM C311. 28 day	

Table 3.4 The properties and moisture content of aggregate

Specification	Fine aggregate	Coarse aggregate
Size range	0-5	5-15
Free weight (SSD)	2.62	2.71
Water absorption	1.21	0.39

3.2.2 Coating Mixture Design

In this study, three types of blends were used with mineral additives. The water cement ratios in the blends used vary between 0.3-0.58 and the binding cement ratio is between 0.04-0.07.

The blends of the mineral mortar for coating are shown in Table 3.5. The properties of silica fume (S.F) and grand ground granulated blast furnace slag (GGBFS) used in coating are shown in Table 3.6.

Table 3.5 The coating mixture

Material	**K1 (Kg/m3)**	**K2 (kg/m3)**	**K3 (kg/m3)**
Cement	900	675	450
S.F	270	202.5	135
Quartz powder (0-0.1mm)	278	293.65	333.18
Quartz sands (0-0.4mm)	252	266.19	302.02
Quartz sands (0.6-1.2mm)	252	266.19	302.02
GGBS	0	225	450
F.A	0	0	0
Water	270	254.42	238.85
S.P	36	33.92	31.85
W/C	0.3	0.38	0.53
S.P/C	0.04	0.05	0.07
Air			
Total	2258.00	2216.88	2242.92

Table 3.6 Properties of supplementary cementitious material used in coating

Chemicals analysis %	S.F	GGBFS
SiO_2	92.26	39.62
Al_2O_3	2-5	11.54
Fe2O3	1-2.5	1.50
CaO	1-2	33.28
MgO	4-8	7.60
Na_2O	-	0.3
K_2O	-	1.02
SO_3	-	0.55
Cl	-	0.0246
Cr_2O_3	1-4	-
C	1-1.5	-
S	0.5-1.3	0.64
Loss on ignition	<5	2.95
Free CaO %	-	0.13

3.2.3 Steel

All blends made in concrete design. City tap water was used. Can be found in some ions and impurities found in city water. In order to influence electro-chemical corrosion measurement devices, city tap water was used in all concrete mixtures, reinforcement was used in reinforced concrete elements based on TS 708 WC III-a class in reinforced concrete elements (Yiğiter, 2008) the yield strength of the reinforcement 487.4 MPa, a tensile strength of 598.1 MPa and an elongation of 21% are the values for which the chemical composition of the steel used is presented in Table 3.7.

Table 3.7 The chemical composition of steel

Component	Quantity (%)
Si	0.19
Mn	0.7
P	0.02
S	0.024
Cr	0.09
Ni	0.11
Cu	0.53
Mo	0.016
Sn	0.02
N	0.011
Pb	0.002
Fe	98.08
C	0.2

In order to determine the corrosion behavior of steel reinforcement used, tests were performed using electrode system. The potential current curve was obtained by using anodic polarization method in the potential scanning curve. The potential growth rate was 0.2 V curvature between -0.2 V and 0.2 mV / s. However, when the potentiostatic capacity is used in the third and fourth stage (1000mA), that is, the test analyzer is automatically terminated when the result of the test stage reaches 1000. The resulting polarization curves are presented in Figure 3.1.

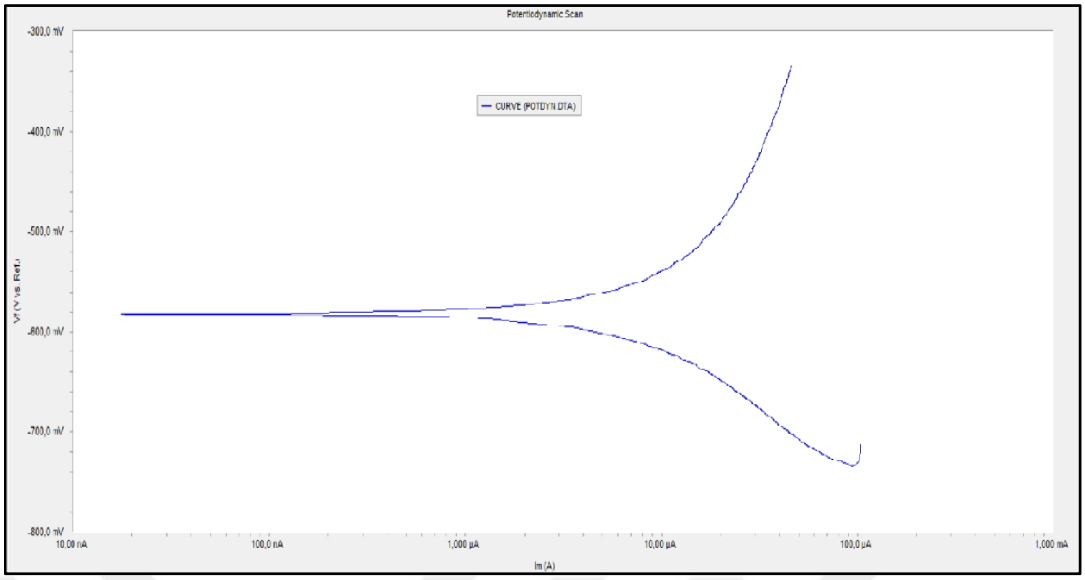

Figure 3.1 Polarization curve

As a result, Tafel analysis, corrosion potential Ecore = -456 mV, corrosion current Icore R = 8.66 µ, corrosion current density icore R = 4.31 µ / cm^2, anodic Tafel constant β a = 74.3 mV cathodic Tafel constant 18c = 188, 6mV, B = 23.14mV.

3.2.4 Preparation Of Specimens

The preparation and corrosion analysis of concrete samples were carried out on 70x70x160 mm prismatic samples. The steel reinforcement is 200 mm long, free of rust and placed 2 cm inside the concrete mat. Plastic filler was used in the sample casting to form the upper part and the horizontal reinforcement. The ends of the steel reinforcement are such that the upper 30 mm of the concrete base is 160 mm long. The preparation step of the concrete example shown in Figure 3.2.

Figure 3.2 Concrete specimens detail and casting (Personal archive, 2016)

3.2.5 Coating Application

In coating applications, the three types of coatings are used, the proportions and types is shown in Table 3.5. Consistency and workability ratio is 28-29 cm, shown in Table 3.5. In these applications, the reinforcement cleaned with sanding method, and prepared for coating, coating is carried out with shotcrete method is shown in Figure 3.4, shotcrete method was applied to a total of 0.75 mm thick by 3 times. Various different samples taken from the same mixture and then cured under the same conditions, we're ready to test samples. The coating sample sizes as round diameter 100 mm and a width of 50 mm were cast. Shown in Figure 3.5.

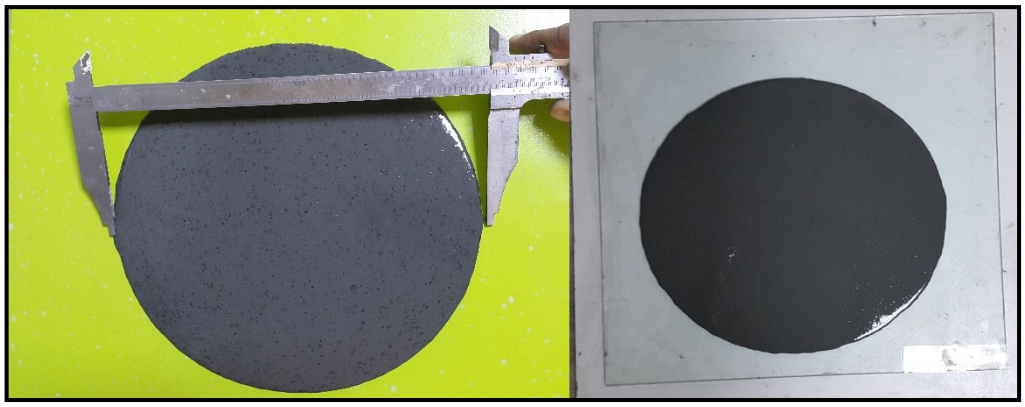

Figure 3.3 Workability Consistency (Personal archive, 2016)

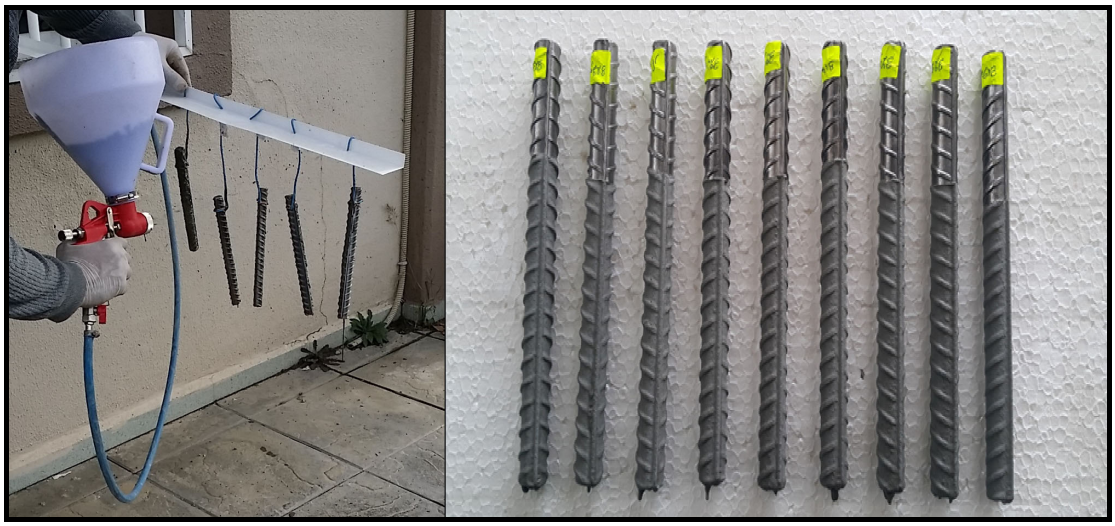

Figure 3.4 Coating application with shotcrete method (Personal archive, 2016)

Figure 3.5 Coating sample as a round diameter (Personal archive, 2016)

3.2.6 Cure

After the prepared samples, the samples are cured in 3 sections (water cure, salt cure, air cure). After preparing the prepared concrete samples for 7 days at 15-20 degrees temperature and moisture content BN = 90% is kept in the curing environment. After the samples had hardened, the samples were removed from the molds and aligned on the table to clean the iron area and coated with epoxy, the process shown in Figure 3.6.

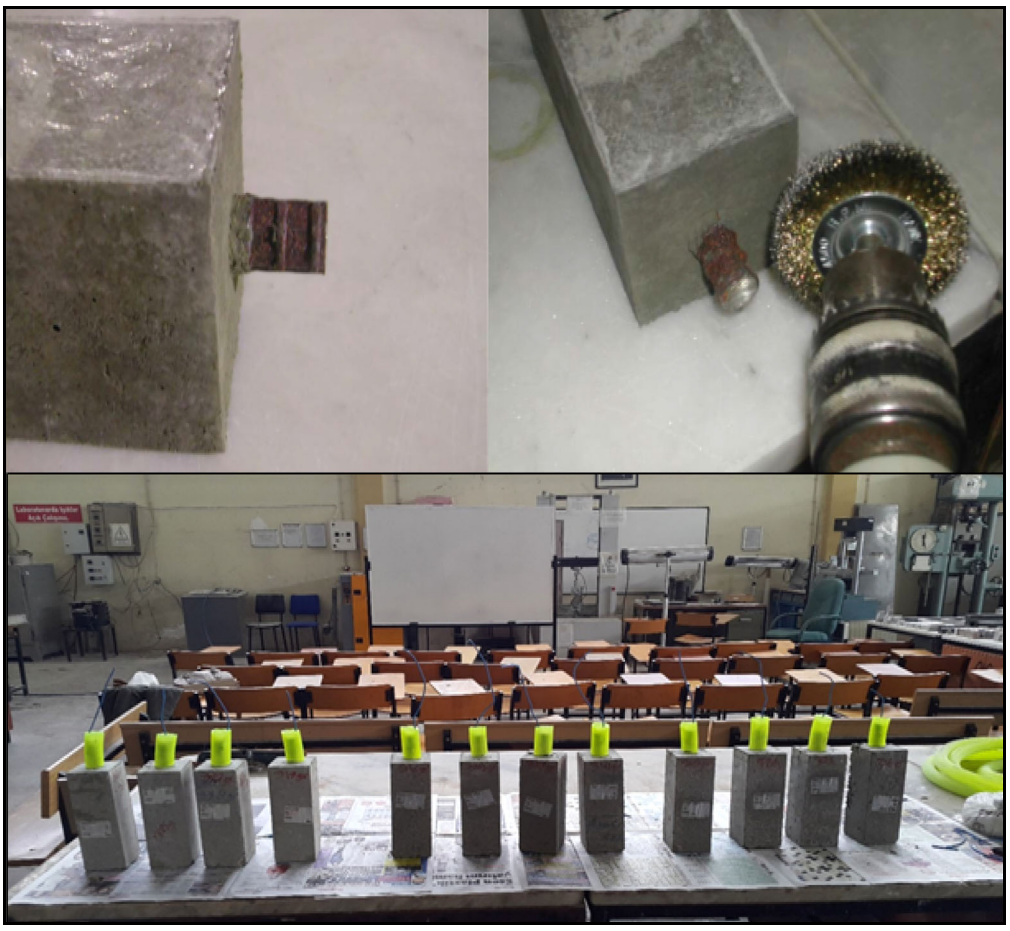

Figure 3.6 Rust cleaning before preparing samples (Personal archive, 2016)

After the epoxy coating was completed, the first 7 day cured specimens were separated for corrosion analysis, the other samples, until it is made of corrosion analysis on the wetting and drying cycling devices for 400 and 800 rpm were stored (See Figure 3.7).

Figure 3.7 Wetting and drying cycle test (Personal archive, 2016)

3.2.7 Corrosion Analysis

Gamry interface 1000 potentiostat is used for corrosion measurement. electrolyte medium in the system, sodium chloride and 3.5% NaCl solution is prepared using pure water. Ambient temperature18-20°C. Reference electrode saturated calomel electrode (SCE) and the counter electrode is graphite. Schematic drawings of the resultant electrochemical cell in figure, the photograph is shown in Figure 3.8.

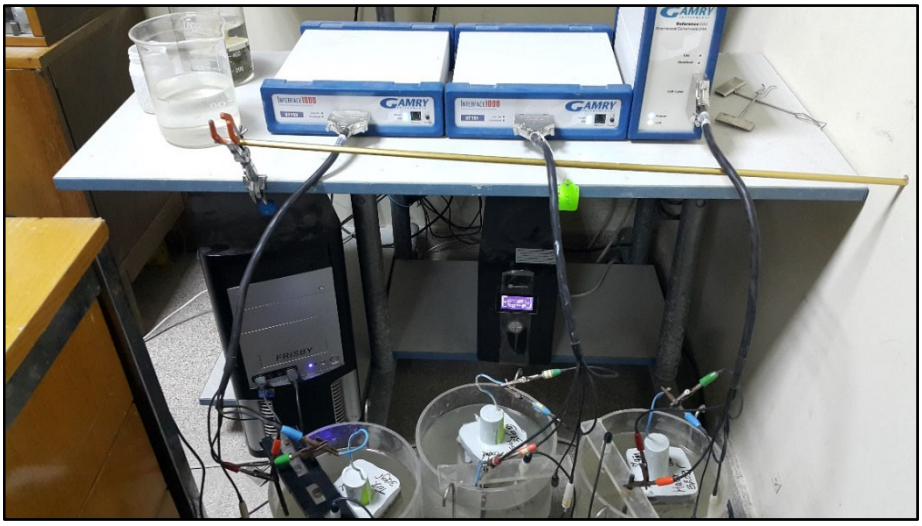

Figure 3.8 The devices used in corrosion analysis (Personal archive, 2016)

In this study, for the rapid corrosion test, open circuit potential was measured at 3600 seconds. Potentiodynamic and Tafel results for the samples measured between -0.2v and 0.2v, and measurement speed 0.2mv / s was evaluated, density 7.87g / cm^3. 1 v application for potetiostatic results were measured up to 72000 seconds. After 400 cycles and 800 cycles wetting and drying for processing, open circuit potential and potentiodynamic results were measured by the same values, only potentiostatic analysis of the performance of the reinforcement coating was not applied, and why, up to 2000 cycles of wetting and drying device is left to hold until samples to deteriorate. Tafel analysis of the electrochemical data acquired as a result of the samples, corrosion potentials (E_{corr}), corrosion current densities (I_{corr}) and corrosion were determined. The Figure 3.9 also shows an example. Tafel analysis with curve and extrapolation performed on the curve is observed.

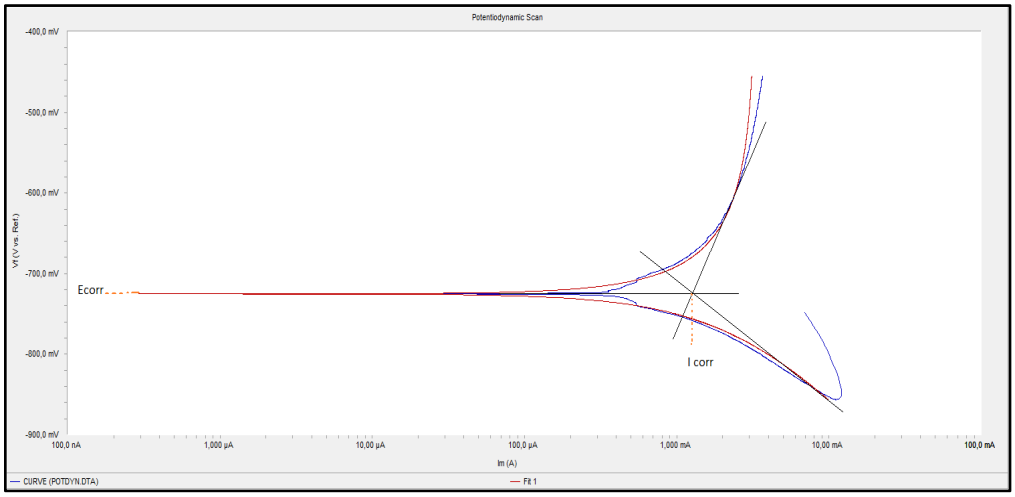

Figure 3.9 Polarization curve and Tafel analysis in reinforced concrete samples

3.3 Inhibitors

All samples were place in concrete with a diameter of 50 mm and a length of 120 mm and were brought in the form of lollipops. The iron rod placed in the concrete is a straight and smooth (8 mm diameter and 140 mm length) bar. Before casting the concrete, the electrodes were polished using a paper carbide sandpaper between 180 and 400 under the fountain to remove the surface. The electrode surface area is only along the longitudinal direction, and is equal to 20.1 cm2 (see in Figure 3.10). The carbon steel reinforcements were place into the specimen according to its longitudinal axis.

Figure 3.10 Reinforced concrete specimens (Personal archive, 2016)

Concrete samples were prepared with a Portland (CEM I 42.5) and natural sand. The water cement ratio (w/c) is 0.5 and the aggregate to cement ratio is 2.8. Two types of mortar are made; one is the control mortar (plain samples) such as the mixing water does not have any inhibitor. For the second one, the di potassium hydrogen phosphate (K_2HPO_4) inhibitor are add to the mortar mixing water, at the content of 0.3-mol/1 kg of cement. The produce mortar is pour into a steel mold and then compact using an air vibrating table during 50 second. After casting, all specimens are keep in air for 24 h, and then cur in water for 7 days.

For flexural and compressive strength tests, mortars are prepare with the same composition previously describe, but using molds (40 x 40 x 160 mm). These mortars are keep in air for 24 h (see in Figure 3.11). Then, they are remove from the molds and store for 28 days in a humid chamber (Temperature of 23 °C).

Figure 3.11 Test specimens for mechanical and corrosion tests (Personal archive, 2016)

3.3.1 Strength Tests

The compressive strength test is performed after the flexural strength test. The compressive strength was specified using a test machine with a load capacity of 3500 KN (ELE) on the broken pieces. The reported test conclusion are the average of five measurements.

3.3.2 Electrochemical Measurements

All tests were specified in a three-electrode cell. (SCE) as control sample, a graphite electrode as auxiliary and the reinforcement rebar in the mortar as working electrode. The corrosion of this study is 3.5 % NaCl solution.

Each samples wear well too many period of electrochemical measurements as following:

(1) Corrosion potential.

(2) Cyclic Polarization.

(3) Anodic polarization at imposed potential OCP ($E_{imposed}$ = 1000 mV/SCE) during 12 h.

Open circuit potential (OCP) of the samples were temperate during 60 min in dipping in chloride solution. The experimental study of potential dynamic polarization were specified at a constant scan rate of 0.1 mV/min.

CHAPTER FOUR
RESULT AND DISCUSSION

4.1 Coating

The electrode potential values of all samples in all three anticipation conditions were measured at various times. Electrode potential values of air cured concrete samples Table 4.1 are given.

Table 4.1 Electrode potential value of air cure

Electrode potential, mV(SCE)	
Samples	**7 Day**
K2 Air cure	-186
K3 Air cure	-286
K1 Air Cure	-166
Control Air Cure	-228

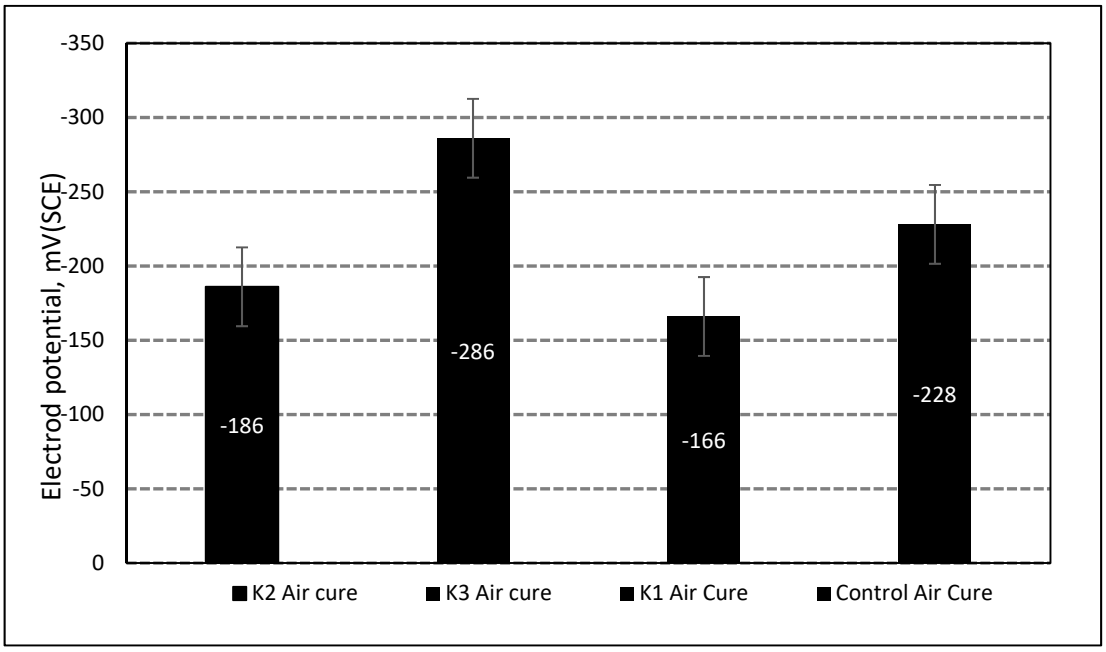

Figure 4.1 Electrode potential value of air cure

When the values in Table 4.1 are considered, electrode potential values are between -20 and -70 mV it is seen. These values indicate no corrosion development according to ASTM C876. Already in the air waiting condition (Air Curing). Since it is known that it is not corrosive, the range of values obtained makes sense. On the other hand, the effective mechanism in air standing condition is the carbonation event. However, the 7-day curing samples that are measured are still at risk of carbonation. It is a result obtained from these measurements.

Table 4.2 Electrode potential values of Water cured concrete samples

Electrod potential, mV(SCE)	
Samples	**7 Day**
K2 Water cure	-159
K3 Water cure	-278
K1 Water Cure	-126
Control Water Cure	-170

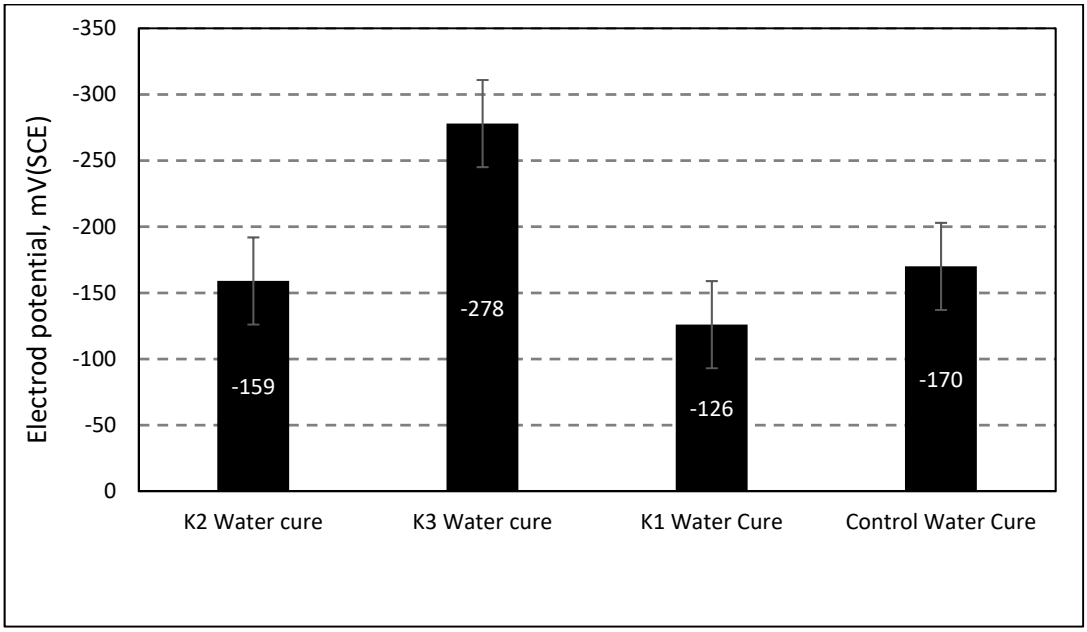

Figure 4.2 Electrode potential values in samples held in water

Electrode potential values between 70 and -257 mV of samples immersed in water it was determined in Table 4.2 Electrode potential values of Water cured concrete samples. Most of the samples were positive for -120 mV and more. Values in the passive region. In some examples (K3 800 cycle – K1 800 cycle), values between -120 and -270 mV fall into the indeterminate class according to ASTM C876. But for values upper than -270 mV the corrosion seems to be start. In general, for values between -120 and -270 there is no active corrosion development in water curing samples (See Figure 4.2).

Electrode potential values of reinforced concrete samples stored in NaCl solution in wetting-drying environment are given in Table 4.3, the graphs for these examples were drawn on the basis of the number of wetting and drying times. The variation of the potential values for the selected mixtures (CTRL, K3, K2, and K1) is given in Figure 4.3. When Table 4.3 is examined, it is seen that the electrode potentials of the samples stored under these conditions are between -68 and -760 mV. Initially, the relatively low measured potential values increased negatively by exceeding -270 mV, the limit of active corrosion development given in ASTM C876 as the number of cycles increased. This increase shows that as the number of wetting-drying repetitions increases, corrosion activity also develops. It should be noted here that the electrode potential values of the rebar according to ASTM C876 can only give an idea as to whether there is corrosion development. It cannot provide information about the rate and intensity of corrosion development.

Table 4.3 Electrode potential values of reinforced concrete samples stored in NaCl solution

Electrod Potential ,mV (SCE)/Cycle			
Samples	**0**	**400**	**800**
Control Water Cure	-170	-623	-725
K2 Water Cure	-159	-354	-562
K3 Water Cure	-278	-289	-573
K1 Water Cure	-126	-329	-395
Control Air Cure	-228	-670	-734
K2 Air Cure	-186	-682	-713
K3 Air Cure	-286	-698	-657
K1 Air cure	-166	-416	-570
Control Salty Cure	-282	-661	-758
K2 Salty Cure	-251	-643	-709
K3 Salty Cure	-305	-656	-701
K1 Salty cure	-229	-512	-595

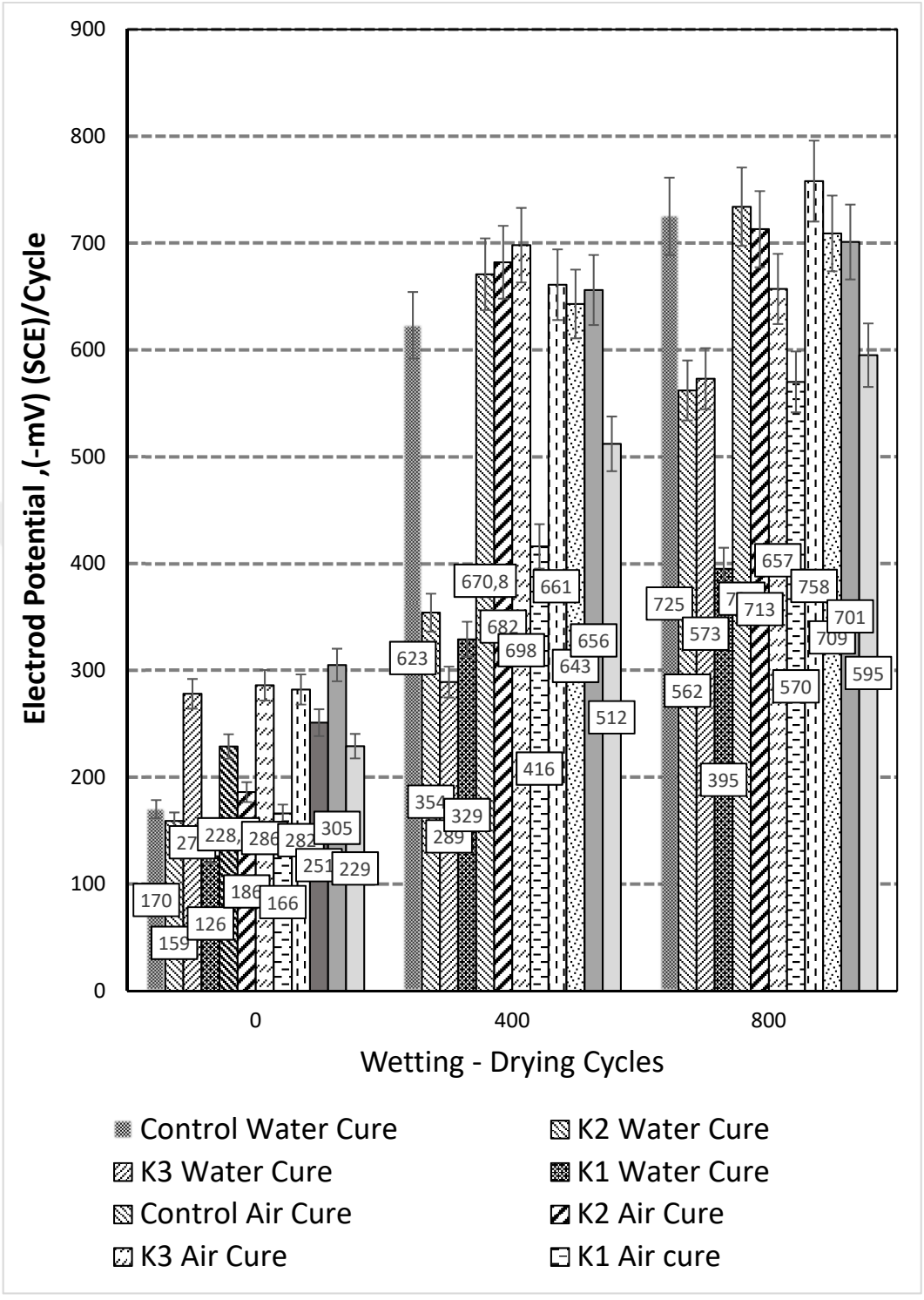

Figure 4.3 Electrode potential values of reinforced concrete samples stored in NaCl solution

The samples prepared with control concretes showed in Table 4.3 potential values between -150 and -300 mV when exposed to wetting-drying effect in 3.5% NaCl solution. The uncoated samples exceeded -270 mV after 400 cycles and entered the active corrosion development zone of ASTM C 876. When compared to the control samples, it was found that the ratio of E_{corr} was closer to zero than the plated samples. However according to ASTM C 876 Active corrosion has been development. When the mixtures were compared, the highest corrosion current density values were obtained in the long run in the samples produced with the control mixture without any precautions. In this case, corrosion current density values reached 4.89 μA / cm^2 at the end of 400 cycles. However, in the experiments, K3, which is high in 50% saline cured samples, was exposed to corrosion by showing side effects in the sample. In samples where K2 was used in the mixture, the current density value was 0.62 μA / cm^2 at 400 cycles. In this case, by using silica fume, the corrosion current density, in other words, the corrosion rate can be reduced by half. It is known that the use of silica fume has improved positively by changing the cavity system of the concrete, on the other hand it has been found that it provides less chlorine accumulation in the reinforcement depth by keeping chlorine ions. These positive effects provide an important benefit in corrosion protection by slowing down the corrosion rate in the reinforcement. However, the fact that silica fume is a much more effective material in terms of pozzolanic and a more impermeable structure with the filling effect of the gap is seen as important benefits in terms of corrosion. Silica fume increases the electrical resistance of concrete, decreases the corrosion current density and delays reinforcement corrosion. On the other hand, in pozzolanic reactions $Ca(OH)_2$ is consumed more quickly and the chemical protection provided by the high alkaline environment is weakened. It is thought that this mechanism is used to obtain relatively less corrosion current density values in slag mixtures compared to slag. Measurement of results of three type of curing samples are given in Table 4.4, Table 4.5 and Table 4.6.

Table 4.4 Corrosion measurement results in concrete that curing in water, with wetting-drying effect in NaCl solution

Sample/Water	Cycles	E_{corr} (mV)	I_{corr} (µA/cm2)
Control	0	-170	0.9395
	400	-623	1.486875
	800	-725	3.983333
K2	0	-159	0.566313
	400	-354	1.24167
	800	-562	2.229167
K3	0	-278	1.013181
	400	-289	1.828333
	800	-573	2.820833
K1	0	-126	0.418933
	400	-329	0.97625
	800	-395	1.3125

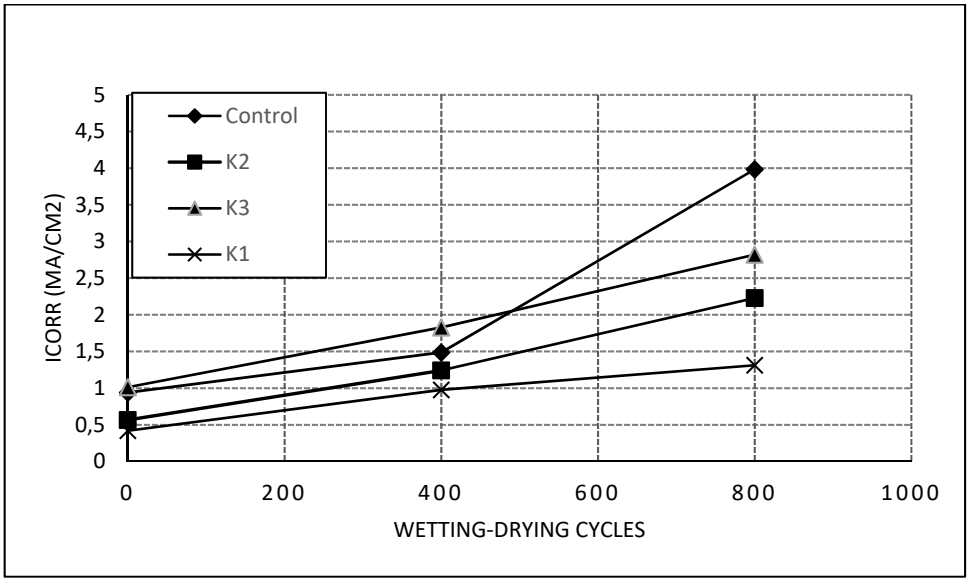

Figure 4.4 Corrosion measurement results in concrete that curing in water, with wetting-drying effect in NaCl solution

Table 4.5 Corrosion measurement results in concrete that curing in air, with wetting-drying effect in NaCl solution

Sample/Air	**Cycles**	**E_{corr} (mV)**	**I_{corr} (µA/cm2)**
Control	0	-228	1.16925
	400	-670	2.483275
	800	-734	4.97453
K2	0	-186	1.228913
	400	-682	2.846257
	800	-713	3.9867
K3	0	-286	1.617881
	400	-698	2.9296533
	800	-657	4.2298633
K1	0	-166	1.69883
	400	-416	2.635925
	800	-570	3.136875

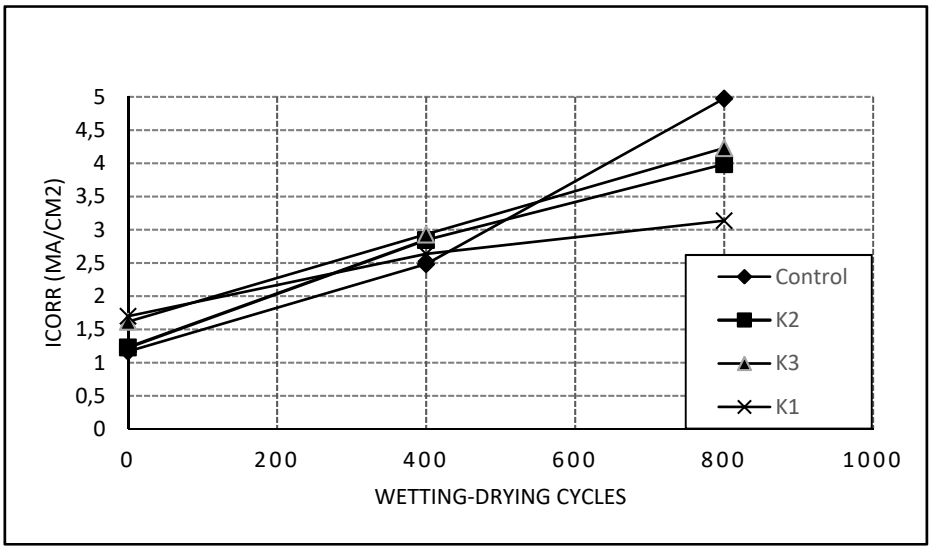

Figure 4.5 Corrosion measurement results in concrete that curing in air, with wetting-drying effect in NaCl solution

Table 4.6 Corrosion measurement results in concrete that curing in salty, with wetting-drying effect in NaCl solution

Sample/Salty	Cycles	E_{corr} (mV)	I_{corr} (µA/cm2)
Control	0	-282	1.93962
	400	-661	2.96575
	800	-758	5.4653
K2	0	-251	1.238963
	400	-643	2.48678
	800	-709	4.763267
K3	0	-305	2.468531
	400	-656	3.022945
	800	-701	4.813683
K1	0	-229	1.345687
	400	-512	2.136545
	800	-595	2.765712

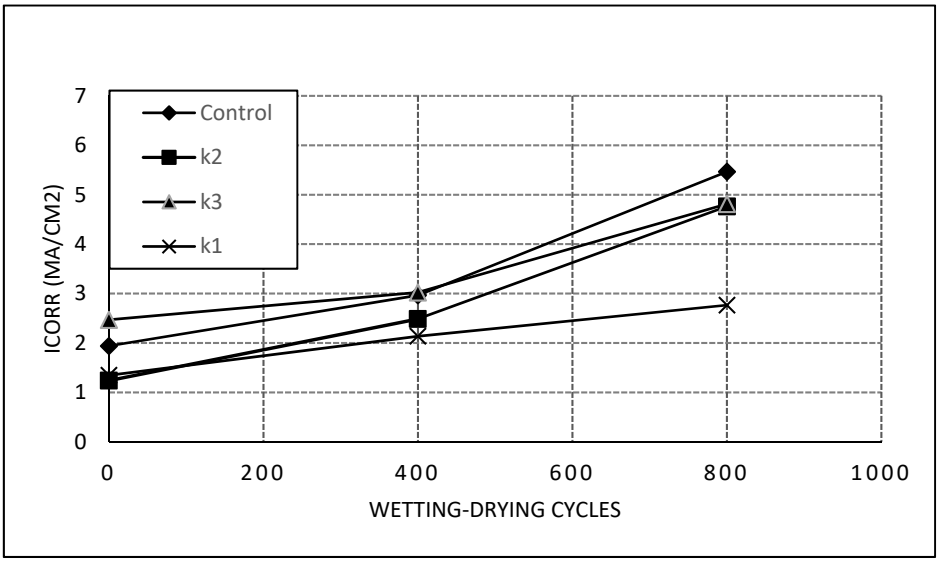

Figure 4.6 Corrosion measurement results in concrete that curing in salty, with wetting-drying effect in NaCl solution

The changes in electrode potential values of reinforcement in concrete according to the number of wetting-drying cycles are presented showed in Table 4.6. In the samples prepared with control concrete, coating doped concrete, it is seen that the corrosion potential values are between -400 and -750 mV in wetting drying cycles in NaCl solution. In other words, active corrosion development is more than 90% likely. However, the potential values of K1 samples appear to be around -330 mV, this change is estimated depending on the blend mixture and percentage ratio. In the so-called mineral admixtures used, it appears that K3 is exposed to corrosion in more active form using 50 percent. While K2 ratio is used as 25 percent, it seems to be a better result (see Figure 4.7-b).

Considering the corrosion values made in various cures, we observe that the ratios in the water cure are more effective. However, when we look at the air cure, we see that concrete is exposed to corrosion earlier because it is more effective. When we use silica fume as a coating on iron, we see that an impermeable layer is formed and NaCl does not penetrate into the iron layer, whereas when the coatings are coated with new concrete, the water in the concrete continues to cure and becomes more impermeable in the hydration process. Using a coating, we see that a more efficient layer is formed and we obtain a more porous area. As it shows in Figure 4.7-d, using k1 and k2 as we have seen in the study based on the control sample, it has reduced corrosion time to a lesser direction than the normal sample, delayed the corrosion life and reduced the corrosion of the iron in a sense. The polarization curve of samples are shown in Figure 4.7.

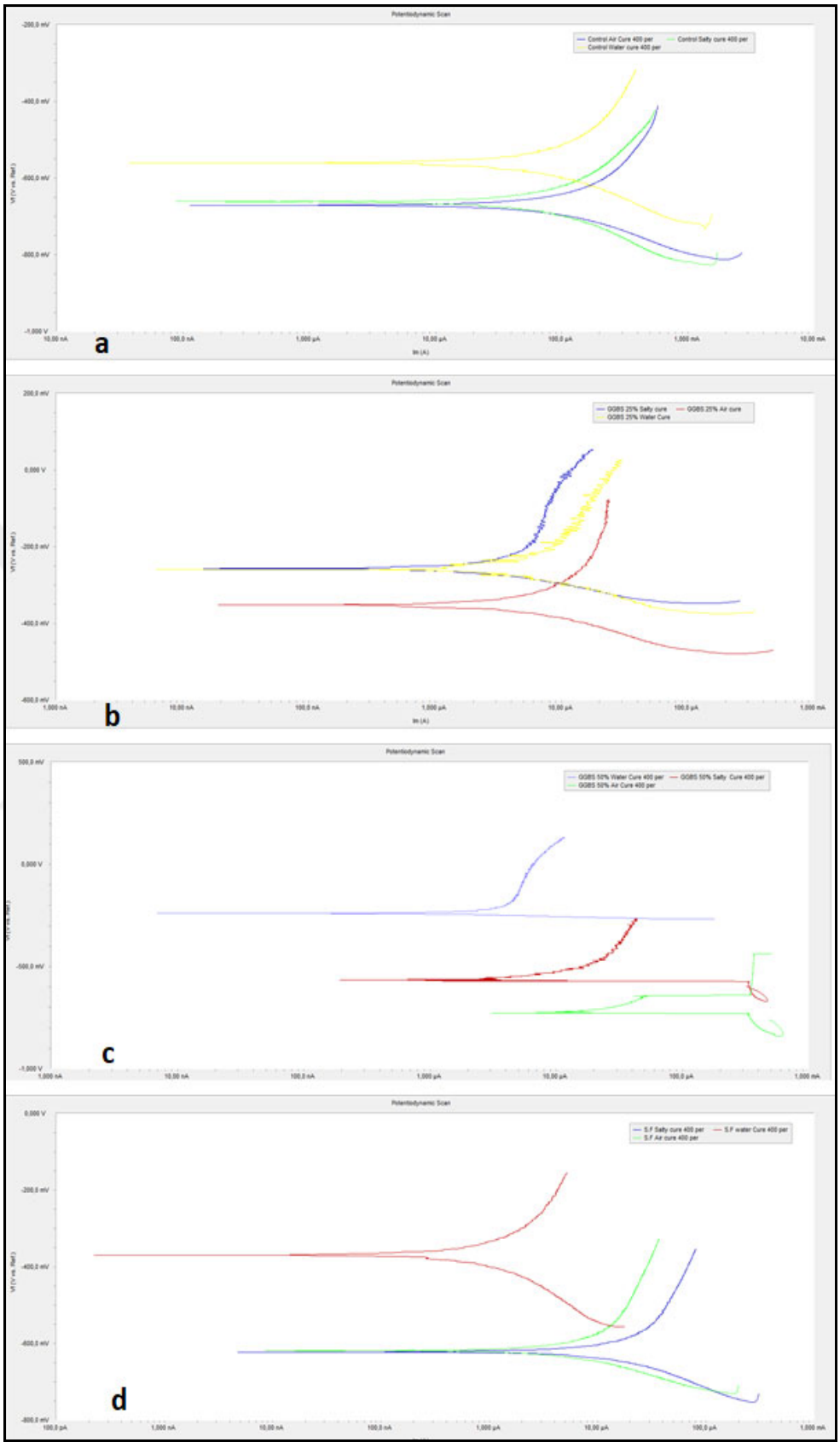

Figure 4.7 Polarization of coating mixture

In terms of rapid chlorine permeability values, permeability values of K3 instead of cement decreased by 87% permeability, by using K2 permeability 60% and 50% K1 sample use decreased fast chlorine permeability values by about 30%. In the initial stages of accelerated corrosion effect, corrosion current density values were very low, while the number of cycles increased, the development of corrosion accelerated. As chlorine ion penetration increased, corrosion rate values increased. This is in good agreement with the two-stage corrosion model.

Increase in porosity values in K3-control samples may lead to these negative results. Observation of uncovered rebar is after electrochemical test showed the severity of the corrosion damage shown in Figure 4.8 and Figure 4.9.

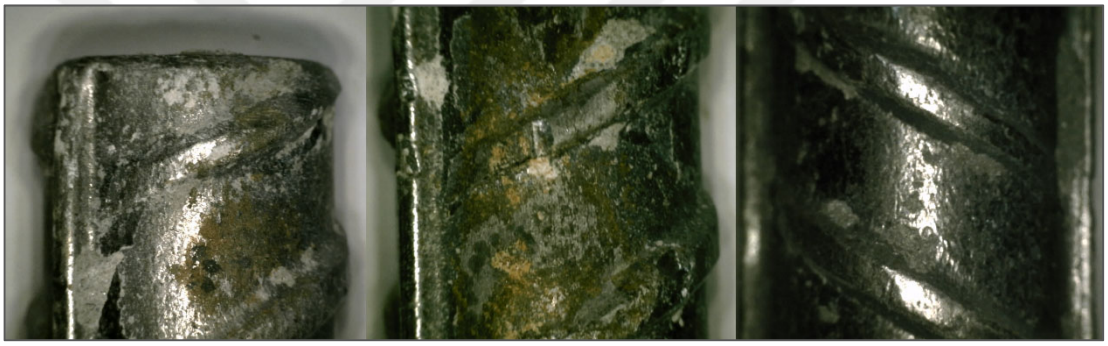

Figure 4.8 From left to right K2, K3, K1 in 400 cycles (Personal archive, 2016)

Figure 4.9 From left to right K3, K1, K2 in 800 cycles (Personal archive, 2016)

4.2 Inhibors

4.2.1 Flexural And Compressive Strengths

The flexural and compressive strengths of the mortars after curing for 28 days and 7 days are shown in Table 4.7 Mechanical results. The addition of phosphate in cement samples has a significant effect on flexural strength. The compressive strength results show a 41-49% reduction in the sample containing the K_2HPO_4 inhibitor compared to the blank sample. This decreases the strength. It is due to the consolidation of the mortar due to its precisely determined set accelerator properties.

Table 4.7 Mechanic test results

Mortar	Flexural Strength 28 Days Cure	Flexural Strength Situ Condition	Compressive Strength 28 Days Cure	Compressive Strength Situ Condition
References mortar		9.84		64.47
Mortar + 0.3 K2HPO4	4.78	9.76	33.87	40.75
Mortar + 0.4 K2HPO4	4.48	7.64	26.71	33.46

4.2.2 Corrosion Measurements

Electrical potential-current graphics obtained from cyclic polarization tests are shown in Figure 4.10 Cyclic polarization curves of specimens Test results indicate an activation of corrosion progress when phosphate inhibitor used in the mortar mix. Furthermore additional increase in activity was observed with the inhibitor dosage of 0, 4 mol/1 kg cement.

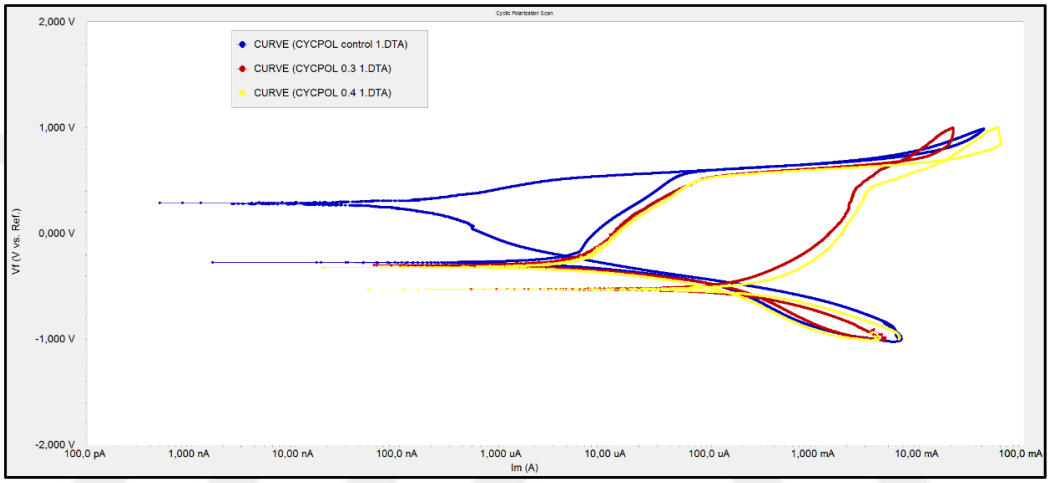

Figure 4.10 Cyclic polarization curves of specimens

Test in the frame of anodic polarization technique at an imposed potential declared similar data. The higher current values can be followed in Figure 4.11.

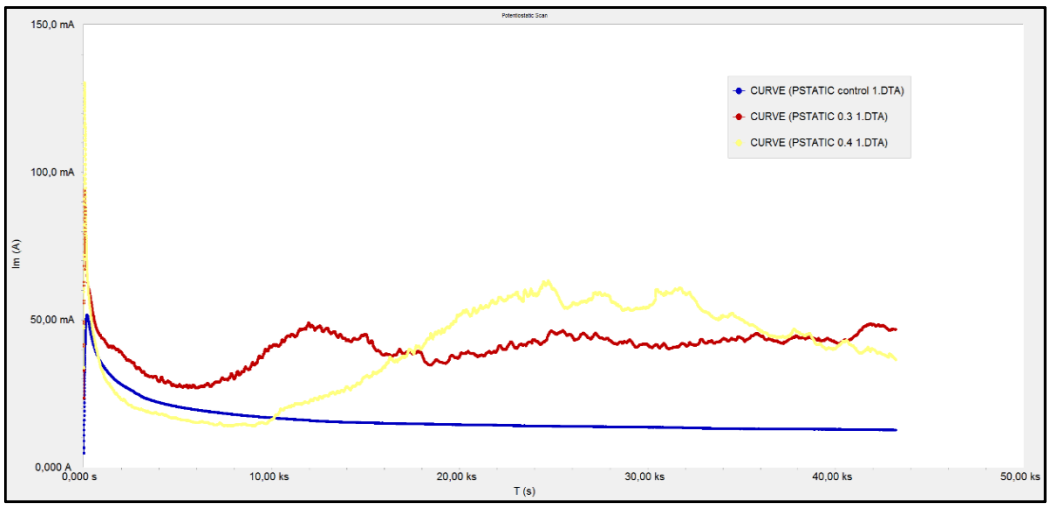

Figure 4.11 Corrosion current values obtained from potentiostatic test

Increase in porosity values by adding phosphate admixture may lead to these negative results. Observation of uncovered rebar's after electrochemical test showed the severity of the corrosion damage (Figure 4.12). Steel rebar in control specimens were protected while the specimens with phosphate added mixture considerably corroded.

Figure 4.12 Steel reinforcement after electrochemical tests (Personal archive, 2016)

4.2.3 Admixture Effectiveness

The effectiveness of the questionable admixture was determined by putting rods into the

- 3.5 % K_2HPO_4,
- 3.5 % NaCl,
- 3.5% NaCl - 1.75% K_2HPO_4 and
- 3.5% NaCl - 3.5% K_2HPO_4

Solutions (Figure 4.13) and the results shown in Figure 4.14.

Figure 4.13 Steel rods in various phosphate and chloride environments (Personal archive, 2016)

Within the whole immersion time steel bars embedded in K_2HPO_4 solution were completely protected. Corrosion damage of rebars in 3.5% NaCl - 1.75% K_2HPO_4 and 3.5% NaCl - 3.5% K_2HPO_4 solutions were minor. Consequently K_2HPO_4 and can be stated as a weak inhibitor with strong side effects (Tiriki, 2003).

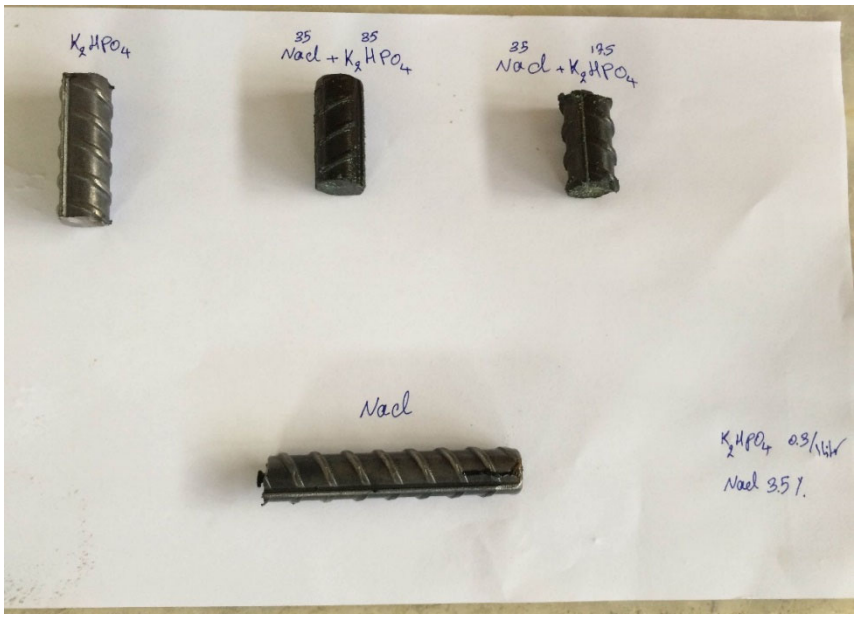

Figure 4.14 Steel rods after exposure to phosphate and chloride environments (Personal archive, 2016)

CHAPTER FIVE
CONCLUSION

Within the scope of this thesis, the development of chloride corrosion, which is highly effective in reinforced concrete structures, is discussed in terms of concrete components and concrete production technology. The use of two types of mineral admixtures in rebar coatings, various curing methods applied to concrete, steel coating insulation applications in terms of corrosion and the effects of the thickness of fixed rust layer on the development of chloride corrosion in reinforced concrete structures were investigated.

There are rare studies in terms of concrete components in studies where corrosive effects and measurement techniques are frequently examined. Corrosion development has not been evaluated in terms of curing method applied to concrete in previous studies. It is thought that the presented study will help these needs in terms of various curing applications and building materials in the construction site environment.

The discussion of the application criteria of various electrochemical methods in the literature is generally made on the experimental data applied with impressed potential and impressed current techniques. In this study, no forced current or potential applications were applied to the samples during the corrosion effect process. The samples were accelerated, but many repetitive natural aging processes were applied in a special laboratory environment with aging equipment. Contrary to the commonly used methods in the literature, in this study, the samples were exposed to the chloride effect caused by the environment around the sea and the development of free corrosion was evaluated.

It is hoped that the polarization technique applied for the evaluation of corrosion developments will support the studies to build up knowledge in the literature. Measurement of corrosion rate values with anodic polarization technique performed by potential screening yields successful results.

Discussion of the application criteria of various coating methods in the literature is generally done with epoxy based coatings. In this study, cement based mineral coating were applied to the samples. In contrast to the epoxy methods commonly used in the literature, the samples in this study are compatible with the environmental condition and evaluated with curing period in the construction site.

Another feature taken into consideration during the planning phase of the study is the study of real-life reinforcements and relatively large samples. In previous studies, it was generally preferred to use small mortar samples and fine diameter reinforcement. In this respect, it is thought that the results of the study will be important.

In this thesis, the results of the experimental studies presented in the relevant chapters are summarized as follows:

• Polarization method used by scanning anodic potential with three electrode system gives very suitable results for determination of corrosion rate values in different coating samples.

• All corrosion rate values obtained from samples lime saturated in water are negligible or very low. This is an expected result in this non-corrosive environment.

• In the initial stages of accelerated corrosion effect, while the corrosion current density values were very low, corrosion development accelerated as the number of cycles increased. As chlorine ion penetration increased, corrosion rate values increased. This is in good agreement with the two-stage corrosion model. However, the corrosion current density values appear to be high in the initial stages and indicate that they are also caused by spraying when evaluated.

• The use of mineral additives in coatings reduced corrosion current density values at the beginning and in the long term in a corrosive environment (NaCl wetting-drying).

• As both silica fume and blast furnace slag dosage increase, fast chlorine permeability values decrease significantly. The changing gap structure and increasing resistivity provide this positive behavior.

• Waiting in the air and wetting-drying conditions in 3.5% NaCl environment reduce the pH values of the reinforcement depths of the samples expected in 0.8-1.0 unit saline water 1.5-2.0 unit within 1 year. While the effective mechanism in air-standing condition was carbonation, in saline water, during the hydration stage, NaCl resulted in a crystallization and porous surface and chlorine ions decreased pH values under wetting-drying effect.

• Corrosion development has been observed in reinforced concrete samples in air, water and salt water. Looking at the development of electrode potential values over time, there is a tendency towards more positive and more negative values than certain negative values. This tendency is an indication that reinforcements become both passive and negative and become more stable over time.

• When the samples prepared with control concrete are examined, it is seen that the corrosion event which is negligible in the initial stage and which develops at low speeds increases to medium and high corrosion rate levels starting from the 400 cycle.

• The use of mineral additives slows down the development of corrosion. In the case of different curing applications, corrosion development was accelerated up to K3 usage in cement based coatings. When K2 sample uses the optimum ratio of 25% in all curing methods, corrosion development is slowed down.

• Characteristic feature of reinforcement exposed to chloride corrosion is local corrosion development and pitting corrosion development.

• Physical protection is more effective than chemical protection. Both the permeability reduced with mineral additives and the protection provided by the

increase in the thickness of the cover are much more beneficial in terms of corrosion performance.

• The addition of K_2HPO_4 admixture in cement specimens has negative effect on its mechanical properties. The porosity of the specimens increased by admixture addition. The admixture could form a protective film on the surface of rods. Evaluation of the mechanical properties of the mortar made by evaluating the mixture properties. However, further investigation is needed to investigate the effect of K_2HPO_4 in understanding the exact mechanism based on other properties, such as pore structure, volumetric behavior, and hydrate compound production. All of the experimental researches related to the subject use vary depending on the percentage, but the inhibitors used in the experiments carried out in normal liquid form observe corrosion resistance. When used in concrete, it shows that the inhibitors become more porous by disrupting the mechanical properties of cement and that the rebar becomes unprotected.

In this study, the accelerated natural aging process applied in the samples to provide corrosion development had a severe effect. Correlation of this severe effect with real-life corrosive effect in terms of chloride corrosion may provide healthier recommendations for reinforced concrete construction processes.

In the experimental studies, no load or stress application was performed on the reinforced concrete samples exposed to corrosive effect. Research on stress corrosion should be carried out in order to determine the levels, as it is predicted that the reinforcement will show more severe corrosion development under stress.

In order to prevent or delay the corrosion, continuation of the works, revitalizing the effect in the publications and construction sites in the past to date, and the development of high performance materials and corrosion should always be given importance.

REFERENCES

Alonso, M. C., Luna, F. J. and Criado, M. (2019). Corrosion behavior of duplex stainless steel reinforcement in ternary binder concrete exposed to natural chloride penetration. *Construction and Building Materials*, *199*, 385–395.

Batis, G. and Rakanta, E. (2005). Corrosion of steel reinforcement due to atmospheric pollution. *Cement and Concrete Composites*, *27*(2), 269–275.

Berrocal, C. G. *et al.* (2015). Corrosion initiation in cracked fibre reinforced concrete: Influence of crack width, fibre type and loading conditions. *Corrosion Science*, *98*, 128–139.

Binici, H. *et al.* (2008). The use of pumice as a coating for the reinforcement of steel against corrosion and concrete abrasions. *Corrosion Science*, *50*(8), 2140–2148.

Briz, E., Biezma, M. V. and Bastidas, D. M. (2018). Stress corrosion cracking of new 2001 lean–duplex stainless steel reinforcements in chloride contained concrete pore solution: An electrochemical study. *Construction and Building Materials*, *192*, 1–8.

Elmoaty, A. E. M. A. (2018). Four-years carbonation and chloride induced steel corrosion of sulfate-contaminated aggregates concrete. *Construction and Building Materials*, *163*, 539–556.

Fu, C. *et al.* (2017). Corrosion characteristics of a 4-year naturally corroded reinforced concrete beam with load-induced transverse cracks. *Corrosion Science*, *117*, 11–23.

Ghorbani, S. *et al.* (2018). Improving corrosion resistance of steel rebars in concrete with marble and granite waste dust as partial cement replacement. *Construction and Building Materials*, *185*, 110–119.

Gunasekara, C. *et al.* (2019). Chloride induced corrosion in different fly ash based geopolymer concretes. *Construction and Building Materials, 200*, 502–513.

Güneyisi, E. *et al.* (2009). Estimation of chloride permeability of concretes by empirical modeling: Considering effects of cement type, curing condition and age. *Construction and Building Materials*, *23*(1), 469–481.

Heniegal, A. M., Amin, M. and Youssef, H. (2017). Effect of silica fume and steel slag coarse aggregate on the corrosion resistance of steel bars. *Construction and Building Materials*, *155*, 846–851.

Hou, L. *et al.* (2017). Effect of corrosion on bond behaviors of rebar embedded in ultra-high toughness cementitious composite. *Construction and Building Materials*, *138*, 141–150.

Hou, L. *et al.* (2018). Bond-slip behavior between pre-corroded rebar and steel fiber reinforced concrete. *Construction and Building Materials*, *182*, 637–645.

Hou, L. *et al.* (2019). Corrosion behavior and flexural performance of reinforced concrete/ultrahigh toughness cementitious composite (RC/UHTCC) beams under sustained loading and shrinkage cracking. *Construction and Building Materials*, *198*, 278–287.

Jaśniok, M. and Jaśniok, T. (2017). Measurements on Corrosion Rate of Reinforcing Steel under various Environmental Conditions, Using an Insulator to Delimit the Polarized Area. *Procedia Engineering*, *193*, 431–438.

Jin, M. *et al.* (2019). Fabrication and characterization of pseudo reference electrode based on graphene-cement composites for corrosion monitoring in reinforced concrete structure. *Construction and Building Materials*, *204*, 144–157.

Kashani, M. M., Crewe, A. J. and Alexander, N. A. (2013). Nonlinear cyclic response of corrosion-damaged reinforcing bars with the effect of buckling. *Construction and Building Materials*, *41*, 388–400.

Kobayashi, K. *et al.* (2018). The effects of PE and PVA fiber and water cement ratio on chloride penetration and rebar corrosion protection performance of cracked SHCC. *Construction and Building Materials*, *178*, 372–383.

Liang, C. *et al.* (2019). Chloride permeability and the caused steel corrosion in the concrete with carbonated recycled aggregate. *Construction and Building Materials*, *218*, 506–518.

López-Ortega, A., Bayón, R. and Arana, J. L. (2018). Evaluation of protective coatings for offshore applications. Corrosion and tribocorrosion behavior in synthetic seawater. *Surface and Coatings Technology, 349*, 1083–1097.

Ming, J., Shi, J. and Sun, W. (2018). Effect of mill scale on the long-term corrosion resistance of a low-alloy reinforcing steel in concrete subjected to chloride solution. *Construction and Building Materials*, *163*, 508–517.

Moser, R. D. *et al.* (2019). Crevice corrosion and environmentally assisted cracking of high-strength duplex stainless steels in simulated concrete pore solutions. *Construction and Building Materials*, *203*, 366–376.

Nyrkova, L. *et al.* (2019). Influence of electrochemical destruction products of protective coating on properties of pipe steel in neutral medium. *Materials Today: Proceedings*, *6*, 279–287.

Pachón-Montaño, A. *et al.* (2018). Threshold concentration of chlorides in concrete for stainless steel reinforcement: Classic austenitic and new duplex stainless steel. *Construction and Building Materials*, *186*, 495–502.

Papadopoulos, M. P. *et al.* (2007). Effect of salt spray corrosion exposure on the mechanical performance of different technical class reinforcing steel bars. *Materials and Design*, *28*(8), 2318–2328.

Papadopoulos, M. P. *et al.* (2011). Corrosion of exposed rebars, associated mechanical degradation and correlation with accelerated corrosion tests. *Construction and Building Materials, 25*(8), 3367–3374.

Polder, R. B. and Peelen, W. H. A. (2002). Characterisation of chloride transport and reinforcement corrosion in concrete under cyclic wetting and drying by electrical resistivity. *Cement and Concrete Composites*, *24*(5), 427–435.

Pradhan, B. (2014). Corrosion behavior of steel reinforcement in concrete exposed to composite chloride-sulfate environment. *Construction and Building Materials*, *72*, 398–410.

Ramírez, E., González, J. A. and Bautista, A. (1996). The protective efficiency of galvanizing against corrosion of steel in mortar and in Ca(oH)2 saturated solutions containing chlorides. *Cement and Concrete Research*, *26*(10), 1525–1536.

Shi, J., Sun, W. and Ming, J. (2012). Characterization of corrosion behaviors of steel in concrete by time and frequency domain electrochemical methods. *Procedia Engineering*, *27*(2011) 412–422.

Sun, W. *et al.* (2004). The influence of mineral admixtures on resistance to corrosion of steel bars in green high-performance concrete. *Cement and Concrete Research*, *34*(10), 1781–1785.

Taji, I. *et al.* (2019). Application of statistical analysis to evaluate the corrosion resistance of steel rebars embedded in concrete with marble and granite waste dust. *Journal of Cleaner Production*, *210*, 837–846.

Thomas, M. D. A. and Matthews, J. D. (2004). Performance of pfa concrete in a marine environment - 10-year results. *Cement and Concrete Composites*, *26*(1), 5–20.

Ungaro, M. L., Carranza, R. M. and Rodriguez, M. A. (2012). Crevice Corrosion Study on Alloy 22 by Electrochemical Noise Technique. *Procedia Materials Science*, *1*, 222–229.

Uthaman, S. *et al.* (2019). Enhanced seawater corrosion resistance of reinforcement in nanophase modified fly ash concrete. *Construction and Building Materials,* 232–243.

Wang, W. and Lu, C. (2018). Time-varying law of rebar corrosion rate in fly ash concrete. *Journal of Hazardous Materials*, 520–528.

Wang, Z. *et al.* (2014). Corrosion of rebar in concrete under cyclic freeze-thaw and Chloride salt action. *Construction and Building Materials*, *53*, 40–47.

Wong, H. S. *et al.* (2010). On the penetration of corrosion products from reinforcing steel into concrete due to chloride-induced corrosion. *Corrosion Science,* 2469–2480.

Xi, X., Yang, S. and Li, C. Q. (2018). A non-uniform corrosion model and meso-scale fracture modelling of concrete. *Cement and Concrete Research*, *108*, 87–102.

Xia, D. H. *et al.* (2017). Assessing atmospheric corrosion of metals by a novel electrochemical sensor combining with a thin insulating net using electrochemical noise technique. *Sensors and Actuators, B: Chemical*, *252*, 3–358.

XIA, H., CHEN, Q. and WANG, C. (2017). Evaluating corrosion resistances of Fe-based amorphous alloys by YCr/Mo values. *Journal of Rare Earths*, *35*(4), 06–411.

Zafar, I. and Sugiyama, T. (2018). The influence of bending crack on rebar corrosion in fly ash concrete subjected to different exposure conditions under static loading. *Construction and Building Materials, 160*, 293–307.

Zhang, P. *et al.* (2017). Steel reinforcement corrosion in concrete under combined actions: The role of freeze-thaw cycles, chloride ingress, and surface impregnation. *Construction and Building Materials*, 113–121.